



Norwegian University of
Science and Technology

DC Tangential Electric Breakdown Strength of Silicone Rubber Interfaces under dry, wet and oily conditions

Ole Andre Hammerøy

Master of Science in Electric Power Engineering

Submission date: June 2016

Supervisor: Erling Ildstad, ELKRAFT

Co-supervisor: Emre Kantar, ELKRAFT

Norwegian University of Science and Technology
Department of Electric Power Engineering

NORGES TEKNISK-NATURVITENSKAPELIG UNIVERSITET



Hovedoppgave våren 2016

Student: Ole André Hammerøy (ole.hammeroy@hotmail.com)

Supervisor: Professor Erling Ildstad (erling.ildstad@elkraft.ntnu.no)

Co-supervisor: Stip. Emre Kantar (emre.kantar@ntnu.no)

Title: *DC Tangential Electric Breakdown Strength of Silicone Rubber Interfaces under dry, wet and oily conditions.*

Tittel: *Tangentiell elektrisk DC holdfasthet til grenseflater mellom silikon gummi i tørr, våt og oljefyllt tilstand.*

This work will be a part of an on-going project at NTNU/SINTEF-Energy Research aiming at developing new criteria for electric design of cable accessories and compact high voltage subsea connectors.

Interfaces between insulating solids are important but also weak parts of many high voltage insulation systems. During service such interfaces can typically be subjected to electric stress, oriented both tangentially and perpendicular to the interface. Experience shows that the breakdown strength particularly is limited by the tangential electric field. Illustrated by the fact that the tangential electric breakdown strength of an interface usually is a fraction of that of pure solid insulation. In addition, the breakdown and partial discharge inception value strongly depends upon the elasticity, surface roughness, contact pressure and type of lubricant applied at the interface.

The main purpose of the project work will be to study and experimentally examine how the DC and AC tangential electric breakdown strength for SiR (silicone rubber) are affected under dry, wet and oily interface conditions.

The work is expected to constitute of:

- A literature survey forming the base for suggested methods and discussion of the results obtained.
- Design and characterization of materials and methods used.
- Experimental examination of the DC tangential electric breakdown strength of the interface connection formed by two silicone rubber specimens under dry, wet and oily conditions.
- Evaluation and discussion of results with respect to contact theory, previous work and proposed activity.
- Conclusions and suggestions for further work
- Suggestions for further work

The details of the test program are to be decided in cooperation with the supervisors.

Start: 18. Januar 2016

Innlevering: 17. Juni 2016

Faglærer: Prof. Erling Ildstad (Erling.Ildstad@elkraft.ntnu.no)

Prof. Erling Ildstad Supervisor

Preface

This master thesis has been performed at the Department of Electric Power Engineering, NTNU, Trondheim, with Prof. Erling Ildstad as main supervisor. The research is part of an on-going project at NTNU/SINTEF-Energy research, aiming at developing new criteria for design of compact high voltage subsea connectors. This research contains a literature study, methods and results from experimental work during spring 2016. This thesis is written for readers with common knowledge within the special field of electric power engineering.

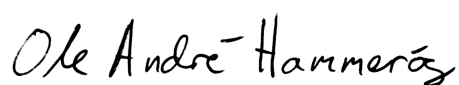
First I would like to thank my supervisor at NTNU, professor Erling Ildstad, head of the Department of Electric Power Engineering, for his guidance and feedback during my research work on my master thesis.

I would also like to thank associate professor Frank Mauseth for the help obtaining the equipment needed for my experimental setup and guidance during my experimental work at the NTNU's laboratories.

Finally I would like to thank Stip. Emre Kantar for his great help during my experimental work and teaching me the laboratory skills needed for my results both for my specialization project and master's thesis.

O.A.H.

Trondheim, June 2016



Ole André Hammerøy

Summary

This research work is a part of an on-going project at NTNU/SINTEF-Energy Research aiming at developing new criteria for design of compact high voltage subsea connectors.

Most high voltage insulation systems consists of interfaces between different solid insulators consisting of different materials. These interface connections are exposed to high voltage electric stresses either parallel or perpendicular to the surface.

The aim of this paper has been to investigate the tangential DC breakdown strength for silicon rubber (SiR) under dry, wet and oily interface connection conditions. This to identify how the breakdown strength are influenced by these conditions under DC voltage.

Existing research has examined the same conditions under AC voltage. These results have been used for comparison as a foundation to understand the difference between the tangential breakdown strength of these interfaces for AC and DC voltages.

The tangential electric breakdown strength of SiR has been examined using laboratory facilities and over 300 hours of HV DC experiments has been run. This has lead to comparable results showing the characteristics for the tangential electric breakdown strength for SiR under dry, wet and oily interface conditions.

Simulations examining the enhanced electric field strength inside the voids in the interface connection has been made using Comsol Multiphysics 5.1. This to see how the electric field strength was influenced by the different interface conditions under AC and DC voltage. The simulations has been used as a foundation to interpret the experimental breakdown strength results.

The results for dry interface condition has shown that the difference between AC and DC under such condition has a breakdown strength in the same range.

The results for wet interface conditions showed that the water filled voids acted as contaminations at the interface connection providing high electric fields in the voids. For AC conditions this lead to a rapidly decomposition of the material interface causing a breakdown strength 3.5 times lower for AC than for DC.

The results for oily interface conditions showed that the oil and the SiR are such good dielectric materials that are quite similar. This lead to a high breakdown strength in the same area, only deviating due to minor differences between the permittivity and conductivity characteristics. This gave the oily interface condition a very strong tangential breakdown strength compared to the dry and wet conditions.

The estimated breakdown voltage (EBDV) has been calculated using contact theory and compared to the experimentally results for AC and DC dry interface conditions. The EBDV has been calculated using two different composite elasticity modulus E_1 and E_2 . It has been performed to reveal the impact of elasticity modulus on the break down voltage (BDV) both theoretically and experimentally as well as to show the agreement between theory and experiments. The results showed that the contact theory was not reliable for estimating the interfacial breakdown voltage for dry interface conditions. It was not able to reveal the impact of the elasticity modulus when the results estimated the best fit breakdown voltage using the elasticity modulus that was 4 time higher than the experimentally measured value for SiR.

Sammendrag

Dette forskningsarbeidet er en del av et pågående prosjekt ved NTNU / SINTEF-Energiforskning med mål om å utvikle nye kriterier for utforming av kompakte høyspent undervanns-kontakter.

De fleste høyspennings isolasjonssystemer består av grenseflater mellom forskjellige faste isolatorer som består av forskjellige materialer. Disse grensesnitt-forbindelsene er utsatt for høye elektriske påkjenninger, enten parallelt eller vinkelrett på overflaten.

Målet med denne oppgaven har vært å undersøke silikongummiens tangentielle elektriske DC holdfasthet med tørre, våte og oljefylt grensesnitt-forbindelser. Dette for å identifisere hvordan den elektriske holdfastheten påvirkes av disse forholdene under likespenning.

Eksisterende forskning har undersøkt de samme forholdene under vekselspanning. Disse resultater er blitt anvendt for sammenligning som et grunnlag for å forstå forskjellen mellom den elektriske holdfastheten for AC og DC-spenninger.

Den tangentielle elektriske holdfastheten for silikongummi har blitt undersøkt ved hjelp av laboratoriefasiliteter, og over 300 timer med HV DC eksperimenter har blitt kjørt. Dette har ført til sammenlignbare resultater som viser silikongummiens elektriske holdfasthet ved de forskjellige forholdene.

Den elektriske feltstyrken som oppstår i hulrom har blitt simulert ved bruk av COMSOL Multiphysics 5.1. Dette ble gjort for å se hvordan den elektriske feltstyrken påvirket de ulike grensesnitt-forholdene under AC og DC spenning. Simuleringene har vært brukt som et grunnlag for å tolke de eksperimentelle elektrisk holdfasthet resultatene.

Resultatene viste at ved tørre grensesnitt-forhold hadde AC og DC tangentiell elektrisk holdfasthet i det samme området.

Resultatene for våte grensesnitt-forhold viste at vannfylte hulrom fungerte som forurensninger i grensesnittets tilkobling. Dette gav høye elektriske felt i deler av hulrommene. For AC forhold fører dette til en hurtig nedbrytning av materialet i grensesnittet som forårsaket elektrisk holdfasthet 3,5 ganger lavere for AC enn for DC.

Resultatene for oljeaktige grensesnitt-forhold viste at oljen og silikon gummi er gode dielektriske materialer som har ganske like dielektriske egenskaper. Dette fører til en høy elektrisk holdfasthet i det samme område, bare avvikende på grunn av små forskjeller mellom permittivitet og konduktivitet. Dette ga oljet grensesnitt en meget høy elektrisk holdfasthet i forhold til de tørre og våte grensesnitt-forholdene.

Den estimerte elektriske holdfastheten er beregnet ved hjelp av kontakt-teori, og sammenlignet med eksperimentelle resultater for AC og DC under tørre grensesnitt-forhold. Den estimerte elektriske holdfastheten er beregnet ved hjelp av to forskjellige komposittelastisitetsmoduler $\acute{E}1$ og $\acute{E}2$. Det har blitt utført for å vise virkningen av elastisitetsmodulen på den elektriske holdfastheten både teoretisk og eksperimentelt, så vel som å vise overensstemmelser mellom teori og eksperimenter. Resultatene viste at kontakt-teorien ikke var pålitelig for beregning av elektrisk holdfasthet for tørre grensesnitt-forhold.

Abbreviations

NTNU Norwegian University of Science and Technology

SINTEF Foundation for Scientific and Industrial Research

SiR silicone Rubber

PD Partial Discharge

BDV Breakdown voltage

EBDV Estimated breakdown voltage

Contents

- Preface I
- Summary II
- Sammendrag IV
- Abbreviations VI

- 1 Introduction 1**
- 1.1 Background 2
- 1.2 Objectives 2

- 2 Literature review 3**
- 2.1 Dielectric polarization 4
- 2.2 Basic electric theory 5
- 2.3 Time dependent polarization 6
- 2.4 Contact theory 7
- 2.5 Estimation of the interfacial breakdown voltage 10
- 2.6 Elasticity modulus 11
- 2.7 Electric field distribution 12
- 2.8 Partial discharges 14
- 2.9 AC - Tangential electric breakdown strength 15

- 3 Methods 17**
- 3.1 Assumptions for the contact theory 18
- 3.2 Setup for electric breakdown testing 19
- 3.3 Procedure for electric breakdown testing 20
- 3.3.1 Procedure for dry interface 20
- 3.3.2 Procedure for oily interface 20

3.3.3	Procedure for wet interface	21
3.3.4	Preparation of experiments	21
3.3.5	Execution of experiments	22
3.4	Production of silicone rubber specimens	23
3.5	Surface preparations	24
3.6	Determining the polarization time constant τ	25
3.7	Procedure for elasticity modulus testing	26
3.7.1	Tensile method	26
3.7.2	Compression method	27
3.8	Estimation of the interfacial breakdown voltage	28
4	Results	29
4.1	Elasticity modulus for silicone rubber	30
4.2	Estimated interfacial breakdown voltage	30
4.3	DC - Tangential electric breakdown strength	31
5	Discussion	33
5.1	Elasticity modulus for silicone rubber	34
5.2	Estimated interfacial breakdown voltage	35
5.3	AC vs. DC - Tangential electric breakdown strength	36
5.3.1	Dry interface - AC vs. DC	36
5.3.2	Wet interface - AC vs. DC	38
5.3.3	Oily interface - AC vs. DC	40
6	Conclusion	43
A	Electric field distribution simulations using Comsol Multiphysics 5.1	49
A.1	Dry interface conditions AC vs. DC plot	50
A.2	Dry interface conditions AC vs. DC graph	51
A.3	Wet interface conditions AC vs. DC plot	52
A.4	Wet interface conditions AC vs. DC graph	53
A.5	Oily interface conditions AC vs. DC plot	54
A.6	Oily interface conditions AC vs. DC graph	55

Chapter 1

Introduction

1.1 Background

Interfaces between insulating solids are very important but also weak parts of any high voltage insulation system. During service such interfaces are typically subjected to electric stress, oriented both tangentially and perpendicular to the interface. Experience shows that particularly the tangential electric field, limits the breakdown strength of these connections between insulation materials. This is illustrated by the fact that the tangential electric breakdown strength of an interface usually is a fraction of what a pure solid insulation is. In addition, the breakdown and partial discharge inception value strongly depends upon the elasticity, surface roughness, contact pressure and type of liquid applied at the interface.

The main purpose of the project work will be to study and experimentally examine how the DC and AC tangential electric breakdown strength for silicone rubber (SiR) is affected under dry, wet and oily interface conditions. Existing research regarding the same conditions under AC voltage will be used as a basis for comparison.

1.2 Objectives

- Define the polarization time constant τ for silicone rubber.
- Experimentally examine and define the elasticity modulus E for silicone rubber.
- Define the estimated breakdown strength of silicone rubber using contact theory.
- Experimentally examine the DC tangential electric breakdown strength of the interface connection formed by two silicone rubber specimens under dry, wet and oily conditions.
- Compare DC results to existing AC results under influence of these conditions.
- Compare the estimated breakdown strength of SiR to experimentally results examining the reliability of contact theory and elastic modulus results.

Chapter 2

Literature review

2.1 Dielectric polarization

A dielectric material like SiR consists of bounded electric charges. These charges are randomly oriented when there is no electric field applied. When applying an electric field over the dielectric material, the dipoles starts aligning in the same direction as the field. This phenomena is called polarization and is in the electric theory divided into four types of polarization mechanisms:

1. **Electronic polarization:** When the electric field is applied to an atom the electrons surrounding the nucleus are influenced. This makes the electrons displaced and concentrated on one side of the nucleus. The phenomena arise rapidly when the field is applied and returns to its natural when the field is removed.
2. **Ionic polarization:** Molecules consists of positive and negative ions. When applying an electric field the positive and negative ions are pulled in different directions establishing a temporary dipole. The temporary dipole vanish momentary when the electric field is turned of.
3. **Orientation polarization:** Some molecules are permanent dipoles. Water for instance are arranged with a randomly direction without having an electric field applied. When applying an electric field all the molecules will arrange in the same direction as the applied electric field.
4. **Interface polarization:** In dielectric materials the arrangement of atoms, ions or molecules is not perfect. There can also be impurities and cavities forming small surfaces. In addition they can contain some free electrons. When applying an electric field these charges can move through the material and attract to these surfaces. This will create a local electric field. (1)

These four mechanisms contributes to the polarization time constant τ defining how long it takes for a material to fully polarize.

2.2 Basic electric theory

The Electric field between two points can be expressed as in equation 2.1

$$E = -\nabla U \quad (2.1)$$

where E is the electric field and U the potential between the electrodes. By using Gauss law the relation between the electric field and charge q can be found. This can be used to find the relation between the capacitance and the electric field. For a parallel plate capacitor this can be written as in equation 2.2

$$C = \frac{Q}{U} = \epsilon_r \epsilon_0 \frac{A}{d} \quad (2.2)$$

where Q is the total charge, A is the area of the electrode and d is the distance between the elements. ϵ_r is the relative permittivity and ϵ_0 is the vacuum permittivity. From basic theory the conductor resistivity can be written as

$$R = \frac{1}{\sigma} \frac{d}{A} \quad (2.3)$$

where σ is the material conductivity, d is the conductors distance and A is the conductors area. From these equations the polarization mechanism time constant τ can be described as in equation 2.4

$$\tau = CR = \frac{1}{\sigma} \epsilon_r \epsilon_0 = \rho \epsilon_r \epsilon_0 \quad (2.4)$$

Where ρ is the volume resistivity [Ωm].

2.3 Time dependent polarization

The alignment of dipoles in a dielectric material is time dependent by the time constant τ . When an electric field is applied, the two first polarization mechanisms, electronic and ionic polarization will immediately activate, shown in figure 2.1 as AP_m and AE_0E . Then the orientation and interfacial polarization starts described by AP_d . These two polarization mechanisms contributes to the time constant τ given by the extension of the slope describing the materials electric charge.

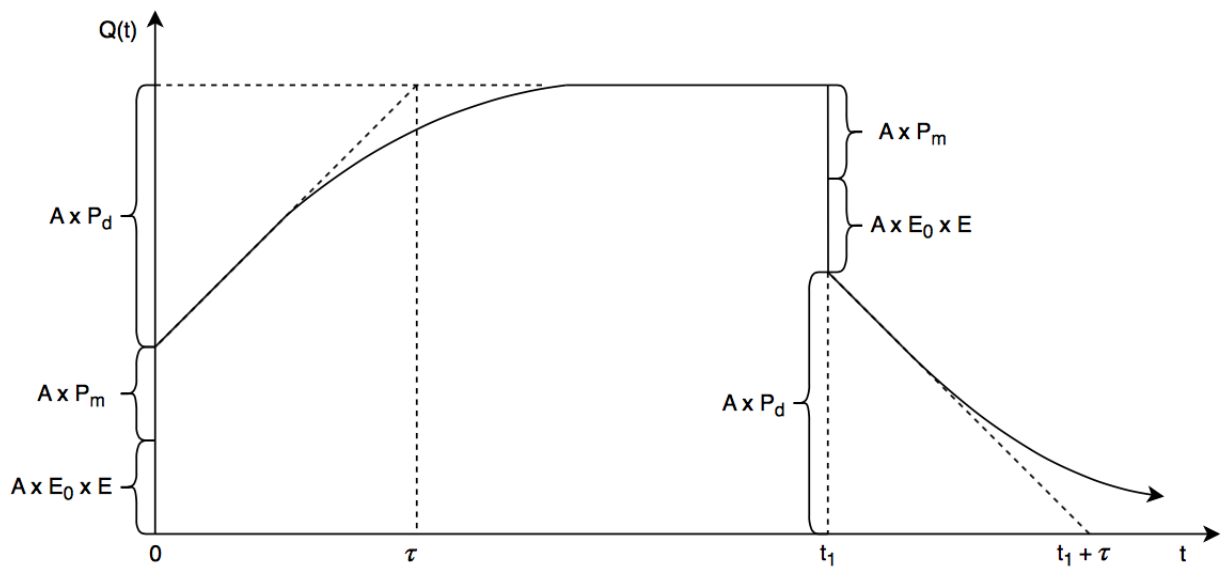


Figure 2.1: Build-up of a charge on a dielectric material showing a step up voltage at $t = 0$ and an electric breakdown at t_1 .

After time τ the material can be assumed as fully polarized and obtained by a stabile DC voltage distribution.

2.4 Contact theory

When making a connection between two solid materials, voids and contact spots are formed at the interface between the two materials, showed in figure 2.2. To reduce the volume of the voids and increase the area of contact spots, mechanical surface pressure can be applied. This could also increase the voids gas pressure. It is reasonable to assume that the surface roughness affect the voids size and units. A coarse surface roughness gives few and large voids, a fine surface roughness gives many and small voids. The voltage applied along the interface will be distributed in a series of connections formed by the voids and contact spots according to equation (2.5)

$$V_i = \sum V_v + \sum V_c \quad (2.5)$$

Where V_i is the applied voltage, V_v is the voltage across a void and V_c is the voltage drop across each contact spot between two voids. Due to the voids low permeability compared to the insulation, electric field enhancement will cause partial discharges activity and accordingly a breakdown of the voids at relatively low voltage. (2)

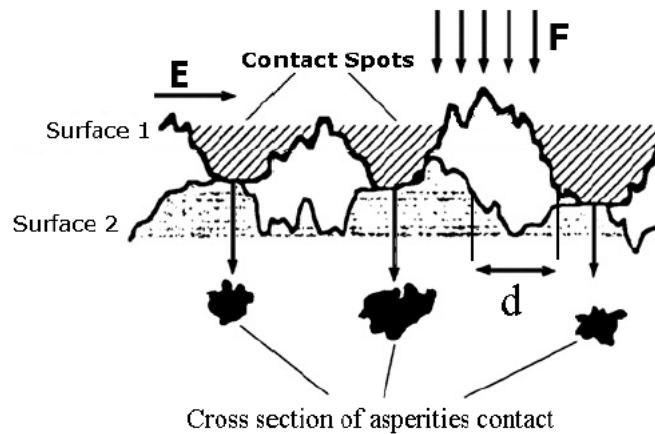


Figure 2.2: Example of a cross-section of the interface between two insulating materials showing cavities and contact spots. (2)

The average diameter d of voids can be expressed by equation 2.6. The voids average diameter is used to calculate the theoretical electric breakdown voltage for SiR interfaces. It is also used to simulate the electric field distribution of the voids simulated by using Comsol Multiphysics. In this thesis three different situations is examined, air, oil and water filled voids,

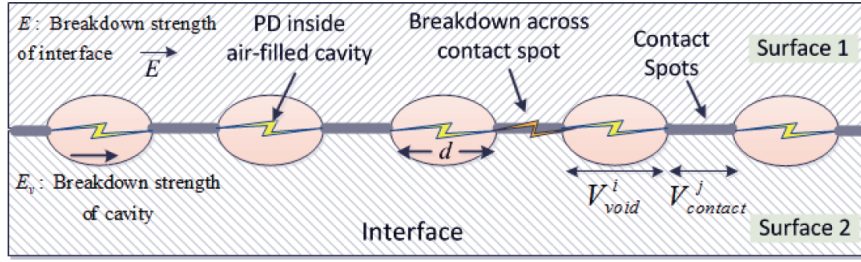


Figure 2.3: Model of the electric distribution along the interface displaying V_{void} and $V_{contact}$. (2)

the simulations are attached in appendix A.

$$d = 2\sqrt{\frac{(A - A_{re})}{n\pi}} \quad (2.6)$$

In order to calculate the average diameter of voids d , three parameters need to be determined, \hat{E} , σ and β where \hat{E} is the composite elasticity modulus determining the materials tensile strength, σ is the standard deviation of peaks height and β is the radius of asperity summits.

Equation 2.7 determines the ratio between real contact area A_{re} and nominal contact A .

$$A_{re}/A \approx 3.2 \frac{p_a}{(\hat{E}\sqrt{\sigma/\beta})} \quad (2.7)$$

Where p_a is the apparent pressure given by $p_a = \frac{F}{A}$ where F is the vertical force pressing the surfaces towards each other and A is the area of the interface.

The number of contact spots at the interface of two mating specimens n is given in equation 2.8.

$$n = 1.21\eta A \left(\frac{p_a}{(\eta\beta\sigma)(\hat{E}\sqrt{\sigma/\beta})} \right)^{0.88} \quad (2.8)$$

The parameters σ , β_m and η are used to solve the equations in the contact theory. They are found in article (3) by Stip. Emre Kantar. The parameters are found using the apparatus *Bruker Contour GT* (4). The system utilizes white light interferometry (WLI) to perform rapid 3D non-contact surface measurements.

From the surface analyze measurements H , W_a , W_s and σ are found. In figure 2.4 the surface

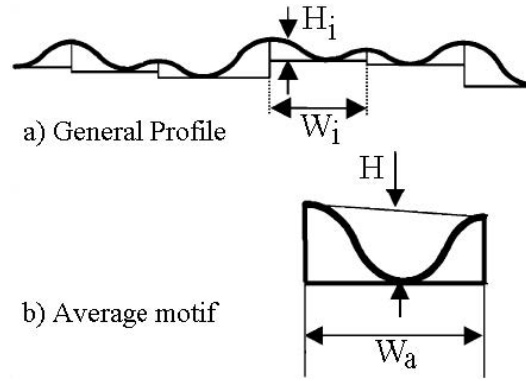


Figure 2.4: Geometrical characteristics of a) a profile; b) an average section of the profile.

analyze measurements are graphically described. These measurements are used to calculate the needed parameters for the contact theory by using equations 2.9 and 2.10.

Where η is the surface density of asperities

$$\eta = 1.2D^2, \quad D = \frac{1}{W_a} \quad (2.9)$$

and β is the radius of asperity summits.

$$\beta = \frac{1}{16} \frac{W_a^2 + W_s^2}{H} \quad (2.10)$$

All the needed parameters are listed in table 2.1.

Table 2.1: Surface roughness parameters

	Value	Description
$\hat{E}[MPa]$	10.7	Composite elasticity modulus
$A_{re}[mm]^2$	0.22	Real contact area
$A[mm]^2$	0.02562	Nominal contact area
$A/A_{re}[\%]$	9.5	Contact ratio
$\sigma[\mu m]$	0.73	Surface characteristics constants
$\beta_m[\mu m]$	2.56	Surface characteristics constants
$\eta[\mu m]^{-2}$	0.1018	Surface characteristics constants
ν	0.58	Poisson's ratio
n	1311	Number of voids
$d[\mu m]$	14	Average diameter of void

2.5 Estimation of the interfacial breakdown voltage

The estimation of the breakdown voltage can be calculated using the discharge inception field strength E_v of voids that is governed by its gas pressure p and size d according to the Paschen law (5).

$$E_v = \left(\frac{p_0}{p}\right) \frac{A}{d^2} + \left(\frac{p}{p_0}\right) B + \frac{C}{d} + \left(\frac{p}{p_0}\right)^{0.5} \frac{D}{d^{0.5}} \quad (2.11)$$

Where $p_0 = 1 \text{ atm.}$, $A = 0.00101[\text{kV/mm}]$, $B = 2.4[\text{kV/mm}]$, $C = -0.0097[\text{kV}]$, $D = 2.244[\text{kVmm}^{-0.5}]$

To calculate the estimated breakdown strength of the SiR interface, the discharge inception field strength is divided by the field enhancement factor for sphere shaped cavities (1).

$$E_{BDrms} = \frac{E_v}{\frac{3\epsilon_r}{1+2\epsilon_r} \sqrt{2}} \quad (2.12)$$

Equation 2.12 is applicable to find the estimate of the breakdown voltage of the SiR specimens interface with air filled voids. This is further discussed section in 5.2.

2.6 Elasticity modulus

The modulus of elasticity E also known as Young's modulus. Young's Modulus is named after the 18th-century English physician and physicist Thomas Young and it is a measure of stiffness of an elastic material. It is used to describe the elastic properties of materials like rubber, metals and plastics when they are stretched or compressed. The elasticity modulus E defines the slope of the objects stress-strain curve in the elastic deformation region. The elasticity modulus will increase with the stiffness of the material.

An object is elastic if it restore to its original shape after distortion.

The elasticity is given by dividing the tensile stress by the extensional strain and is shown in equation 2.13.

$$E = \frac{\frac{F}{A_0}}{\frac{dL}{L_0}} \quad (2.13)$$

In the contact theory the composite elasticity modulus \bar{E} is used. It is calculated from experimentally approached values of the elasticity modulus E for the applicable material. Equation 2.14 expresses the composite elasticity modulus for a combination of two elastic materials with different elasticity modulus. The experiments examined in this paper contains specimens both made of SiR with equal elasticity modulus. The equation can then be simplified as in equation 2.15.

$$\frac{1}{\bar{E}} = \frac{(1 - \nu_1)^2}{E_1} + \frac{(1 - \nu_2)^2}{E_2} \quad (2.14)$$

$$\frac{1}{\bar{E}} = \frac{2(1 - \nu)^2}{E} \quad (2.15)$$

The constant ν is the Poisson's ratio. It defines the longitudinal elastic deformation due to stress to the simultaneous lateral deformation. The Poisson's ratio is dimensionless and positive. For the majority of common materials the Poisson's ratio is in the range between 0 and 0.5 and for silicone rubber 0.48 (6).

2.7 Electric field distribution

When an object is energized it can be characterized as an AC voltage in a transient state. The electric field is governed by the permittivities of the materials and gasses in the object and its interface. Equation 2.16 shows the electric field distribution dependent on the permittivity of the material for AC conditions.

$$E_1 = \frac{\epsilon_2}{\epsilon_1} E_2 \quad (2.16)$$

When the material has been energized equal to the polarization time constant τ , the field distribution is governed by the conductivity of the materials like in equation 2.17. The electric stress over the test object will gradually shift to the material with the lowest conductivity.

$$E_1 = \frac{\sigma_2}{\sigma_1} E_2 \quad (2.17)$$

In table 2.2 the materials conductivities and permittivities used in the experiments in this thesis are listed.

Table 2.2: Material parameters, (7), (8), (9), (10), (11).

Materials	Conductivity σ	Relative permittivity ϵ_r
Air	$5e-15$	1
Water	$5.5e-6$	80
Midel 7137	$6.56e-12$	3.75
silicone rubber	$15.56e-12$	2.8

In figure 2.5 the electric field strength is simulated for an interface with one air filled cavity with an applied voltage of 30[kV]. The interface is shown as a straight horizontal line through the middle of the spherical cavity. At AC conditions the permittivities for the materials are applicable. For DC conditions the conductivity for the material is applicable. As shown by the simulations, the air field cavity in figure 2.5a at AC conditions have a lower field strength than the air filled cavity under DC conditions in figure 2.5b. This is due to the ratio between the permittivities and conductivities at the different voltage situations. In table 2.2 the material qualities are listed. From these values its easier to understand the difference.

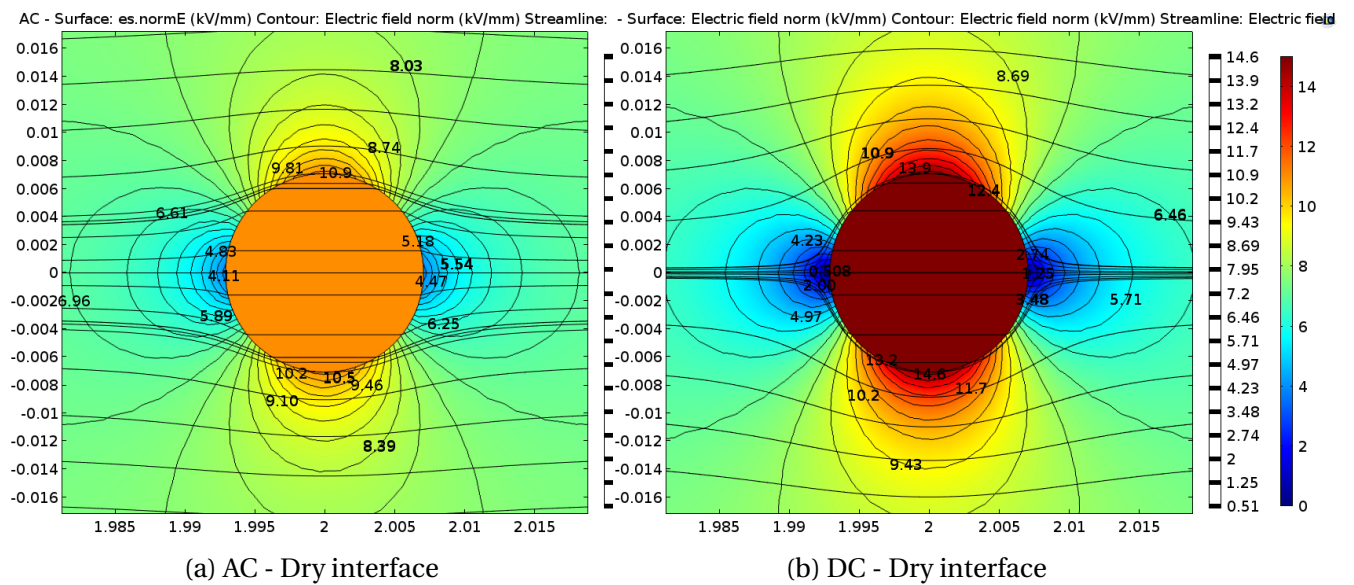


Figure 2.5: Simulated electric field distribution for air filled cavity at the SiR interface [kV/mm]

Simulations for dry, wet and oily interface conditions for both AC and DC are attached in appendix A.

2.8 Partial discharges

Partial discharges will occur in solid, gaseous and liquid insulation materials. Solid dielectrics usually has a higher permittivity than the gaseous dielectrics that has a higher permittivity than the liquid dielectrics. The liquid or gaseous parts of the insulation will have a higher electric stress than the solid insulation. This due to their lower dielectric strength.

The breakdown begins with degradation of the surface or the cavity walls due to partial discharges. This activity contributes to deformation of the indefinite shape of the surface or cavity that later leads to the appearance of electric treeing (1).

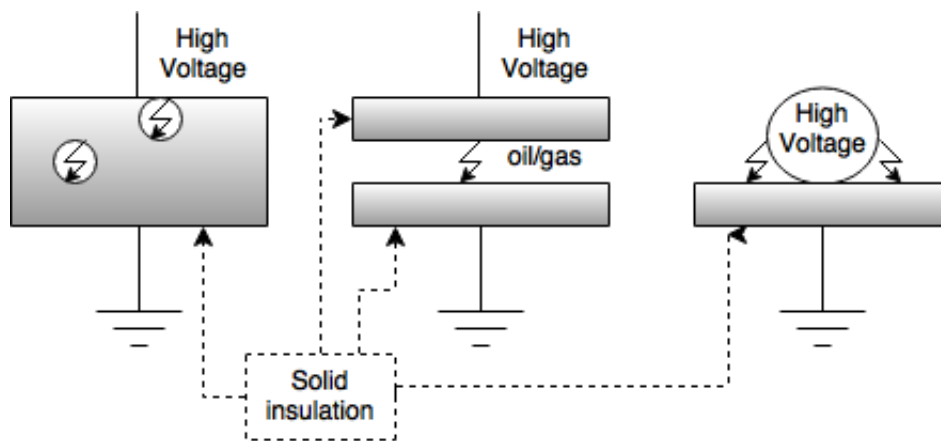


Figure 2.6: Appearance of partial discharges at geometrical constructions

At AC voltage partial discharges will occur two times per period when the amplitude has reached the ignition voltage for the PD activity to start. This will gradually deteriorate the dielectric material until a puncture occurs. This deterioration occurs in three ways:

1. Ions and electrons accelerating in the discharge path causing bombardment of the insulation in the discharge region.
2. Discharges causing chemical reactions in the surrounding materials. This leads to a temperature rise in the PD activity region.
3. Radiations from discharges. Ultraviolet radiation has sufficient energy to break up bonds in organic substances.

2.9 AC - Tangential electric breakdown strength

In this section existing results of the tangential electric breakdown strength for SiR AC voltage is presented. The results is part a part the research Stip. Emre Kantar has examined for silicone rubber under dry, wet and oily interface conditions (12) (13). The results are presented as a Weibull distribution in the same way as the other results in this paper. This to have the same foundation for comparison of the experimental results.

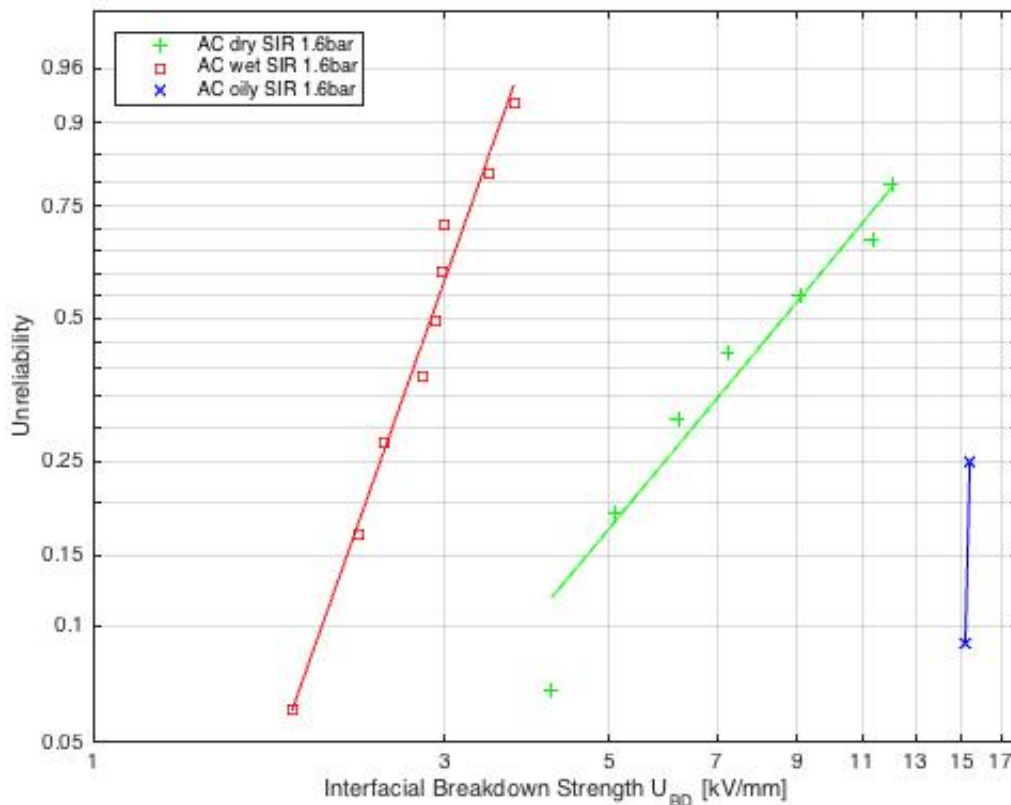


Figure 2.7: Weibull presentation of AC electric breakdown strength with dry, wet and oily interface conditions

Table 2.3: Comparison between dry, wet and oily interface at AC and DC conditions

	U63%	Slope	Min	Max	Mean
Interface	[kV/mm]	a[/]	[kV/mm]	[kV/mm]	[kV/mm]
Dry AC	9.04	2.5	4.18	12.06	7.91
Wet AC	3.07	5.5	1.86	3.72	2.83
Oily AC	15.65	79.1	15.19	15.40	15.30

Chapter 3

Methods

3.1 Assumptions for the contact theory

Following assumptions have been made for using the contact theory for the calculations. It is assumed that the voids have spherical shape and that they are evenly spread on the test objects surface. This means that there is one contact spot between each cavity, this is a continuing pattern covering the whole surface length like in figure 2.2. The air filled voids are assumed vented with a gas pressure of 1 atm. (2). It is also assumed that the surface contains of only elastic contact points.

Three simulations have been done to examine the electric field distribution for wet, dry and oily interface conditions examined in this paper. The simulations have been executed in the finite elements software Comsol Multiphysics 5.1.

3.2 Setup for electric breakdown testing

The existing AC test setup has been rebuilt for DC experiments examining the tangential electric breakdown strength for SiR interfaces. The new DC test setup is explained in this section is shown in figure 3.1.

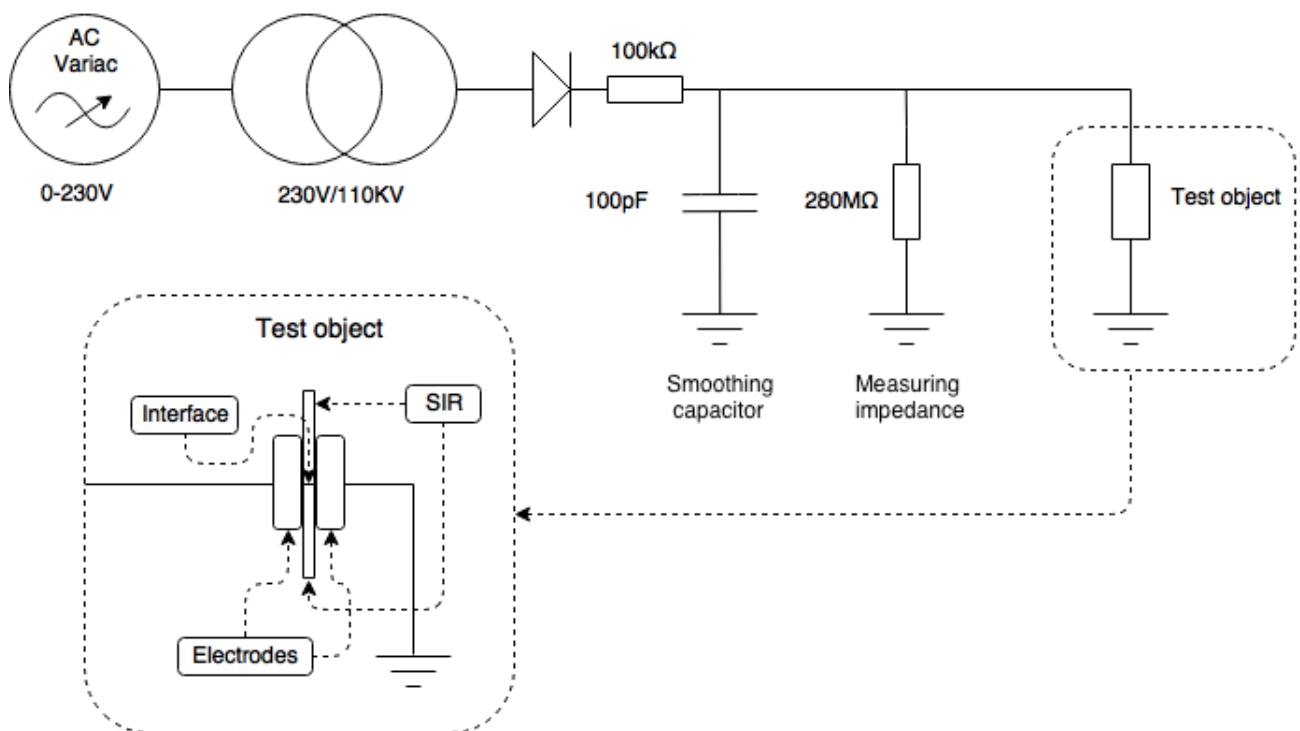


Figure 3.1: Experimental lab setup

The laboratory test setup contains an AC variac source that can carry up 230V 50Hz. It is connected to a transformer with a ratio 230V/110kV. To obtain the wanted DC voltage for the experiments, the AC voltage source is connected to a module based rectifier. The rectifier bridge is then connected to a measuring resistance used for measuring the DC voltage at a lower voltage suitable for the measuring instruments used.

The DC side of the rectifier is then connected to one of the Rogowski plate electrodes shown in figure 3.2. The other ground potential electrode is connected to common earth. The electrodes is mounted in a construction that is called the "test rig" shown in figure 3.2. The test rig is soaked in a container containing the *synthetic ester Midel 7131* (9). This will prevent any unwanted flashover during the experiments and provide that the wanted breakdown happens at the interface of the SiR specimens.

The new DC setup is fully automated using a PLC Programmable Logic Controller for con-

trolling the voltage step ramping every 30 minutes. This due to the polarization time constant τ further explained in section 3.6.

3.3 Procedure for electric breakdown testing

The execution of DC electric breakdown experiments is time consuming due to the polarization time constant τ explained in section 3.6. The test procedure for the DC experiments is explained in this section.

Three different experiments were examined changing only the interface parameter dry, oily or wet mate contact surface. These are further explained in section 3.3.1, 3.3.2 and 3.3.3. Five trials for each experiments were executed to collect reliable results.

Table 3.1: Test parameters

#	Pressure	Paper grit size	Voltage step	Expected BDV	Interface
1	1.6 [bar]	#500	1 [kV] pr. 30min	57.7 [kV]	Dry
2	1.6 [bar]	#500	1 [kV] pr. 30min		Oily
3	1.6 [bar]	#500	1 [kV] pr. 30min		Wet

The expected BDV for the interface can be calculated using the contact theory with the assumptions that the cavities is spherical and air filled. The estimated breakdown voltages are presented in section 5.2.

3.3.1 Procedure for dry interface

The dry interface connection is mated in clean and dry conditions. The SiR specimens are placed in a cleaned test setup without any pressure applied to the interfacial connection. After placing the SiR specimens the weights are applied to achieve wanted interface pressure. It is important to not add any additional pressure when mating the specimens.

3.3.2 Procedure for oily interface

The oily interface connection is made by adding the *synthetic ester Midel 7131* on the surface of the two SiR specimens. This is the same oil used as insulation in the setup. The SiR specimens are placed in a cleaned test setup without any pressure applied to the interfacial connection. After placing the SiR specimens the weights are applied to achieve wanted interface pressure.

3.3.3 Procedure for wet interface

The wet interface connection is made by adding tap water droplets on the surface of the two SiR specimens. They are then mated and cleaned to prevent any water droplets on the outer surface of the specimens. This is to insure there are no water contamination in the oil. The experiments using water at the interface is runned last, to prevent water contamination in the oil for the other experiments examined. The SiR specimens are placed in a cleaned test setup without any pressure applied to the interfacial connection. After placing the SiR specimens the weights are applied to achieve wanted interface pressure.

3.3.4 Preparation of experiments

The preparation for each experiment includes:

- Cleaning the Rogowski plate electrodes with paper, avoiding oil at the surface while inserting the SiR specimens between the electrodes as seen in figure 3.2.
- Insert the SiR specimens, add the applicable weight on top of the rig, making sure the SiR specimens are under the influence of the vertical mechanical weight.
- Lower the rig into the oil filled plastic container.

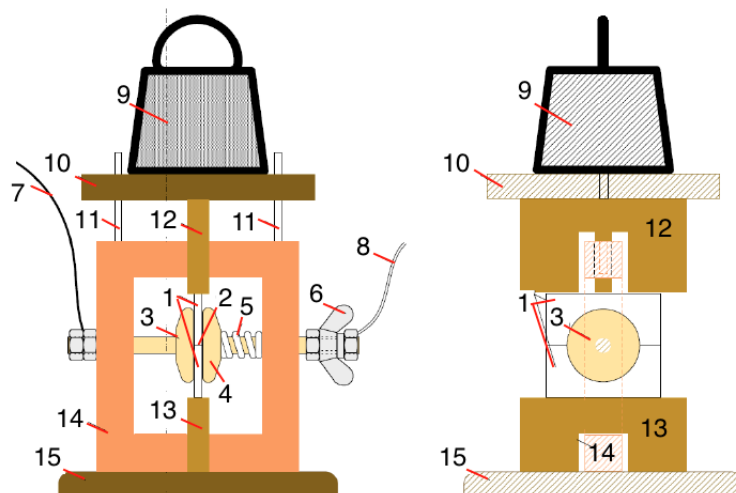


Figure 3.2: Detailed illustration of test rig. 1: rectangular solid SiR specimens, 2: interface, 3: fixed electrode, 4: moving electrode, 5: spring, 6: wing nut, 7: high voltage wire, 8: earth wire, 9: weights, 10: moving weight-carrying plate, 11: guiding rods, 12: moving (upper) pressure dispersing block, 13: fixed (lower) pressure dispersing block, 14: supporting structure, 15: foundation.(6)

3.3.5 Execution of experiments

The execution for each experiment includes:

- Increasing the voltage according to the time constant τ .
- When a breakdown occurs, note breakdown voltage, time and sequence number.
- Confirm that a breakdown has occurred by inspecting the surface of the SiR specimens.
- Mark the specimens with sequence number.
- Mark which specimen was on the top and bottom and which side the HV potential was connected to. This is done if further examination of the breakdown pattern is desired.

3.4 Production of silicone rubber specimens

The SiR specimens were fabricated in laboratory conditions at Sintef polymer laboratory. Using two component SiR Elastosil LR 3003/60 A/B by Wacker Silicones (8). The two components A and B are similar, both transparent and viscous.

The SiR mixture were made by blending the two (A and B) components equal, using an electronic scale figure 3.3 to measure the exact weight of each component. Mixing of the two components were done in clean conditions in a vacuum locker figure 3.4 for two hours. Making sure there is no impurities or cavities in the mix for further preparation. To make the raw formate of the uncut specimens, the mixed SiR where placed in a $4\text{mm} \times 500\text{mm} \times 500\text{mm}$ sized mold like in figure 3.5, and pressed between two steel plates with a pressure of 23 tons and 165°C for 25 minutes. The final hardening where done by putting the raw formate in a oven for 200°C for four hours. To make the final specimens the SiR where cut to $4\text{mm} \times 25\text{mm} \times 55\text{mm}$ sized rectangles like in figure 3.6.



Figure 3.3: Electronic scale with raw SiR



Figure 3.4: Mixing SiR in vacuum chamber

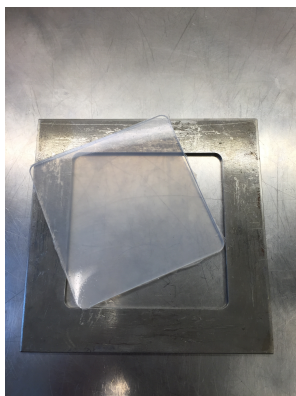


Figure 3.5: Mold $4\text{mm} \times 500\text{mm} \times 500\text{mm}$

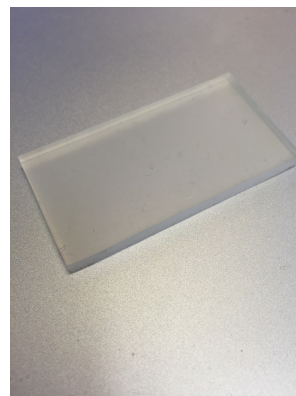


Figure 3.6: Specimen $4\text{mm} \times 25\text{mm} \times 55\text{mm}$

3.5 Surface preparations

The interface surface of the SiR specimens are prepared using the *Struers microprocessor controlled automatic oscillating grinder* (14) at Sintef Laboratories. The specimens are fixed in a disc with capacity of 3 x 5 specimens like in figure 3.7. Figure 3.8 shows the disc connected to the grinder. The circular table below the specimen disc is where the grinding paper is attached. The grinding paper comes in different grit sizes, and is easy to change.

The automatic grinder adds water to the rotating table to remove SiR particles while grinding. It also prevents overheating, melting and deformation of the specimens. The specimens surface are grinded for one minute at 300 rotations per minute. The surface is inspected to see if 100% of the surface is grinded properly, method shown in figure 3.9. After grinding the specimens are cleaned using Isopropanol to remove fat and particles due to grinding.



Figure 3.7: SiR specimens aligned to rotating disc

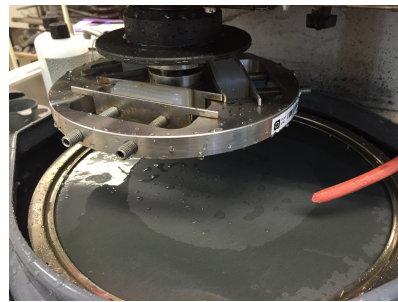


Figure 3.8: Grinding the specimens



Figure 3.9: Surface inspection



Figure 3.10: Specimens bulk

3.6 Determining the polarization time constant τ

The given material parameters found in the product data sheet for the *silicone rubber Elastosil LR 3003/60 A/B* (8) used in the experiments. Values is given at 50Hz at 20°C.

- Volume resistivity $\rho = 5 \cdot 10^{15} [\Omega cm]$
- Relative permittivity $\epsilon_r = 2.8$
- Dielectric strength $U_{bd} = 23 [kV/mm]$
- Dissipation factor $\tan\delta = 20 \cdot 10^{-4}$
- Tensile strength $E_0 = 9,40 [N/mm^2]$

The polarization mechanism time constant τ is given by the equation 3.1.

$$\tau = CR = \frac{1}{\sigma} \epsilon_r \epsilon_0 = \rho \epsilon_r \epsilon_0 \quad (3.1)$$

Inserting the volume resistivity, relative permittivity and vacuum permittivity gives us a time constant τ given in minutes in equation 3.3

$$\tau = \rho \epsilon_r \epsilon_0 = 5 \cdot 10^{13} [\Omega m] \cdot 2.8 \cdot 8.85 \cdot 10^{-12} = 1239 [s] \quad (3.2)$$

$$\tau = \frac{1239 [s]}{60 \left[\frac{s}{min} \right]} = 22 [min], 05 [s] \quad (3.3)$$

In my specialization project (15) two experiments where examined. The aim was to see how DC voltage influenced the tangential electric breakdown strength of the material compared to the existing results for 50Hz AC voltage. The time constants used where $\tau_1 = 1[s]$ and $\tau_2 = 10[s]$. Comparing the calculated time constant τ in equation (3.2) with τ_1 and τ_2 we can see that the earlier test can not be classified as DC experiments with a satisfying DC distribution.

We can classify it as a DC distribution using the calculated time constant in equation (3.2) $\tau = 1239[s]$ for the SiR test objects. This to make sure the polarization mechanisms have completed, and the DC field distribution have stabilized. For the experiments examined in this paper, the time constant τ has been adjusted to 30[min] to make sure the polarization mechanisms have completed.

3.7 Procedure for elasticity modulus testing

The elasticity modulus is measured using the machine *Lloyd LR5K* (16) for tensile and compression testing at Sintef Laboratories. Two different test setups are used, these further explained in 3.7.1 and 3.7.2. The elasticity modulus is examined by running in total seven experiments. One experiment using tensile method and six experiments using compression method. Each experiment consisting of seven trials. The reason for having several compression method experiments is to examine all the conditions regarding surface roughness and applied surface pressure. The tensile method is done by using a standard nomenclature, so a single experiment counting seven trials are sufficient.

3.7.1 Tensile method

The first setup is the most common method and is called tensile testing. It is examined by testing a subject to a controlled tension until failure. Tensile specimens are punched out of the same fabricated SiR used for electric breakdown testing. The dimensions of the test specimen are given in table 3.2 and are graphically shown in figure 3.11.

Table 3.2: Test specimen dimensions

Dimensions	Measure
Overall length	75.0 [mm]
Distance between shoulder	30.0 [mm]
Gage length	20.0 [mm]
Length of grip section	14.0 [mm]
Width of grip section	12.0 [mm]
Width	4.0 [mm]
Depth	4.0 [mm]

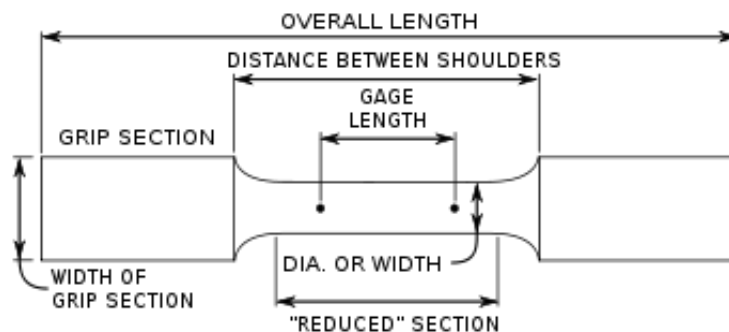


Figure 3.11: Test specimen nomenclature

3.7.2 Compression method

The second method is the compression method. Using two rectangular SiR specimens, with the same dimensions $4\text{mm} \times 25\text{mm} \times 55\text{mm}$ alike the ones used during electric breakdown experiments. The two specimens are placed in composite rack holding them on top of each other. The machine is pressing the two specimens together with a given speed until a given force is reached. The force used in this method is the same as used in the electric breakdown experiments $1.6[\text{bar}]$. This to imitate the conditions the SiR specimens are facing during mating and electric breakdown testing.

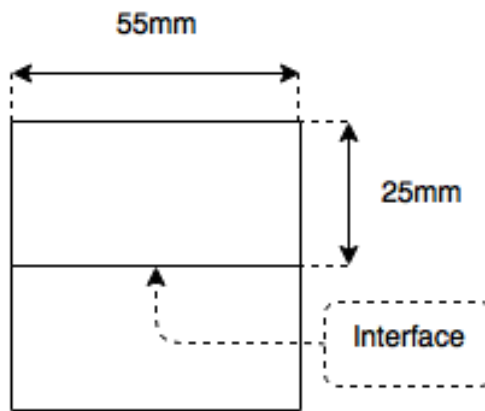


Figure 3.12: Test specimen rectangular

3.8 Estimation of the interfacial breakdown voltage

The estimated breakdown voltage (EBDV) described in section 2.5 is calculated and compared to the experimental results for AC and DC dry interface conditions. The EBDV is calculated using two different composite elasticity modulus \acute{E}_1 and \acute{E}_2 . It is performed to reveal the impact of elastic modulus on the BDV both theoretically and experimentally as well as to show the agreement between theory and experiments. This will give indications of which elasticity modulus E that is reliable and if the contact theory are reliable for estimating the interfacial breakdown voltage for dry interface conditions.

Be aware of the difference between the elasticity modulus E and the composite elasticity modulus \acute{E} .

\acute{E}_1 is based on a experimental approach described in section 3.7 It equals an elastic modulus of $5.77[MPa]$.

$$\acute{E}_1 = 10.7[MPa] \quad (3.4)$$

\acute{E}_2 is found in the paper by previous master student Dimitrios Panagiotopoulos (6). It is the value used in research by both Dimitrios and Stip. Emre Kantar. It is equal to an elasticity modulus of $24.9[MPa]$.

$$\acute{E}_2 = 46[MPa] \quad (3.5)$$

The void diameter in table 4.3 is calculated using the contact theory 2.4 where the composite elasticity modulus \acute{E} is the changing parameter. This is used as a parameter for determining the EBDV.

Chapter 4

Results

4.1 Elasticity modulus for silicone rubber

In this section the experimentally results for the elasticity modulus is presented. The results for compressions testing are given in table 4.1 and for tensile testing in table 4.2.

Table 4.1: Elasticity modulus test parameters and results using compression method

Setup	Weight	Force [F]	Paper grit size	E average
1	1.55 [kg]	15,2 [N]	#500	6.14 [MPa]
2	1.55 [kg]	15,2 [N]	#1000	5.88 [MPa]
3	2,44 [kg]	23,9 [N]	#500	6.29 [MPa]
4	2,44 [kg]	23,9 [N]	#1000	6.29 [MPa]
5	3,65 [kg]	35,8 [N]	#500	5.69 [MPa]
6	3,65 [kg]	35,8 [N]	#1000	6.59 [MPa]
Average value of all trials				6.06 [MPa]

Table 4.2: Elasticity modulus test parameters and results using tensile method

Setup	Velocity	Average E
1	2,28 [mm/min]	5.49 [MPa]

The elasticity modulus E for SiR has been selected by calculating the average of the average values for both stretching and compression method. The experimental approach for the average elasticity modulus for SiR is given in equation 4.1.

$$E_{average} = E_1 = 5.77[MPa] \quad (4.1)$$

4.2 Estimated interfacial breakdown voltage

The calculated EBDV is influenced by the elasticity modulus \acute{E} and the voids diameter d . For \acute{E}_1 the EBDV deviating by 66% from the experimentally results. For \acute{E}_2 the EBDV deviating by 37%. The voids diameter calculated with \acute{E}_1 is nearly 50% smaller then using \acute{E}_2 .

Table 4.3: Estimated electric breakdown strength with respect to the composite elasticity modulus \acute{E}

	\acute{E} [MPa]	Estimated BDV [kV/mm]	Result DC [kV/mm]	Result AC [kV/mm]	Void diamter [mm]
\acute{E}_1	10.7	26.5	7.80	9.04	0.00707
\acute{E}_2	46	14.42	7.80	9.04	0.01394

4.3 DC - Tangential electric breakdown strength

In this section the experimentally results for DC tangential electric breakdown strength for dry, wet and oily interface conditions are presented.

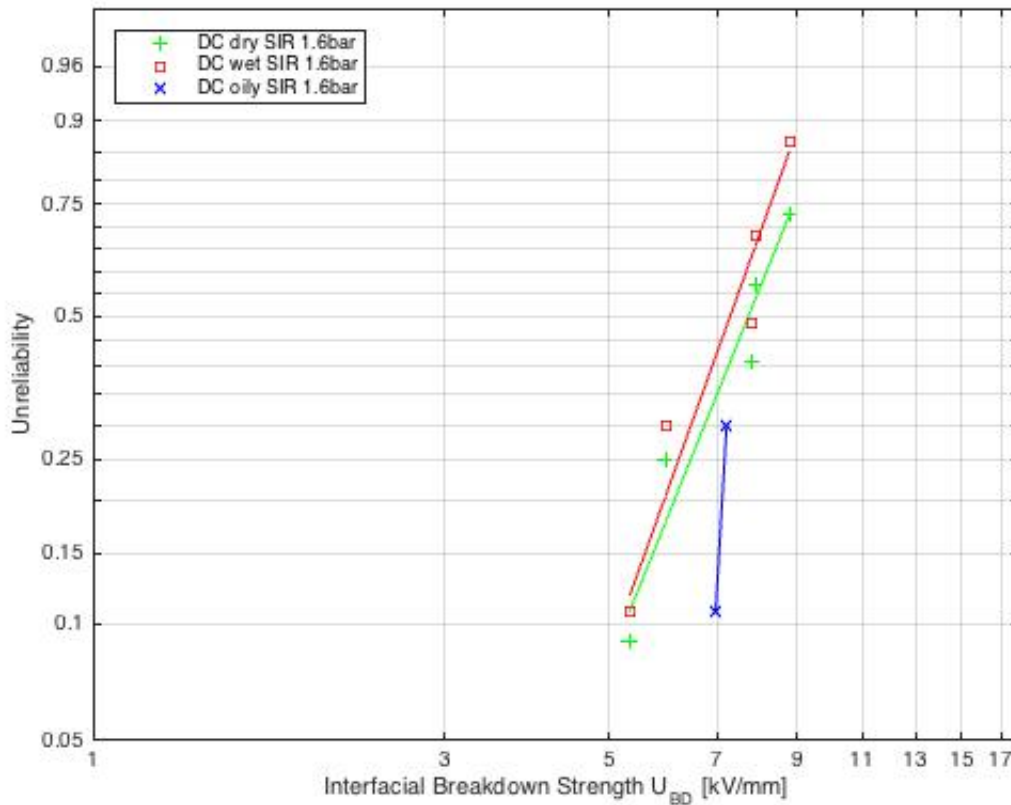


Figure 4.1: DC - Tangential electric breakdown strength under dry, wet and oily interface conditions

Table 4.4: DC - Dry, wet and oily interface conditions

	U63%	Slope	Min	Max	Mean
Interface	[kV/mm]	a[/]	[kV/mm]	[kV/mm]	[kV/mm]
Dry DC	7.80	5.5	5.33	8.78	7.15
Wet DC	10.96	5.1	7.93	11.94	9.57
Oily DC	14.62	33.4	13.70	14.12	13.94

Chapter 5

Discussion

5.1 Elasticity modulus for silicone rubber

The elasticity modulus for the silicone rubber is expected to be $9.4[MPa]$ according to the material data sheet (8). The experimentally approached elasticity modulus resulted in $E_{average} = 5.77[MPa]$.

The experimentally approach of the elasticity modulus for SiR has been found by calculating the average of the average values for both the stretching and compression method experiments. The results gave an average value for the tensile method at $5.49[MPa]$ and for the compression method $6.06[MPa]$. The accuracy of these results are remarkable. Using two completely different methods for measuring the elasticity modulus on the same material in two different shapes.

The difference between the expected $9.4[MPa]$ and the result $5.77[MPa]$ is only by $3.63[MPa]$. The manufacturer of the silicone are using a different test standard than in this paper, this could be the reason for this difference.

The machine had one weakness under tensile testing mode. To measure the materials stretch length a reflex tape is attached at the surface of the SiR test objects. When the test object were being stretched, these reflex tapes moves due to deformation of the test object. Some of the trials were effected and was aborted due to this weakness. For most of the trials this was not an issue.

5.2 Estimated interfacial breakdown voltage

The estimated interfacial breakdown voltage of the SiR interface using the composite elasticity modulus \hat{E}_1 did not correspond to experiment results. The deviation using \hat{E}_1 were as high as 66% compared to the result presented in table 4.3.

Using the composite elasticity modulus \hat{E}_2 the EBDV deviates by 37%. It has a better fit compared to \hat{E}_1 but the composite elasticity modulus is the one that differs the most from both elasticity modulus given by the manufacturer and the experimental approached values. This questions the result regarding the EBDV and the reliability of the contact theory.

The contact theory is dependent on uncertain surface roughness parameters found using the optical surface analyzer. It also contains simplifications that the surface has spherical voids spread evenly on the test objects surface.

According to the research in this paper the contact theory contains to many uncertainties that questions its ability to estimate the breakdown voltage for dry interface conditions.

5.3 AC vs. DC - Tangential electric breakdown strength

In this section the experimental DC results are compared with the AC results from Stip. Emre Kantar presented in section 2.9. Both dry, wet and oily interface conditions are examined to determine how the dielectric material silicone rubber and its tangential electric breakdown strength are influenced by the applied AC and DC voltage.

The red dots describing the AC results and the green dots describing the DC results.

5.3.1 Dry interface - AC vs. DC

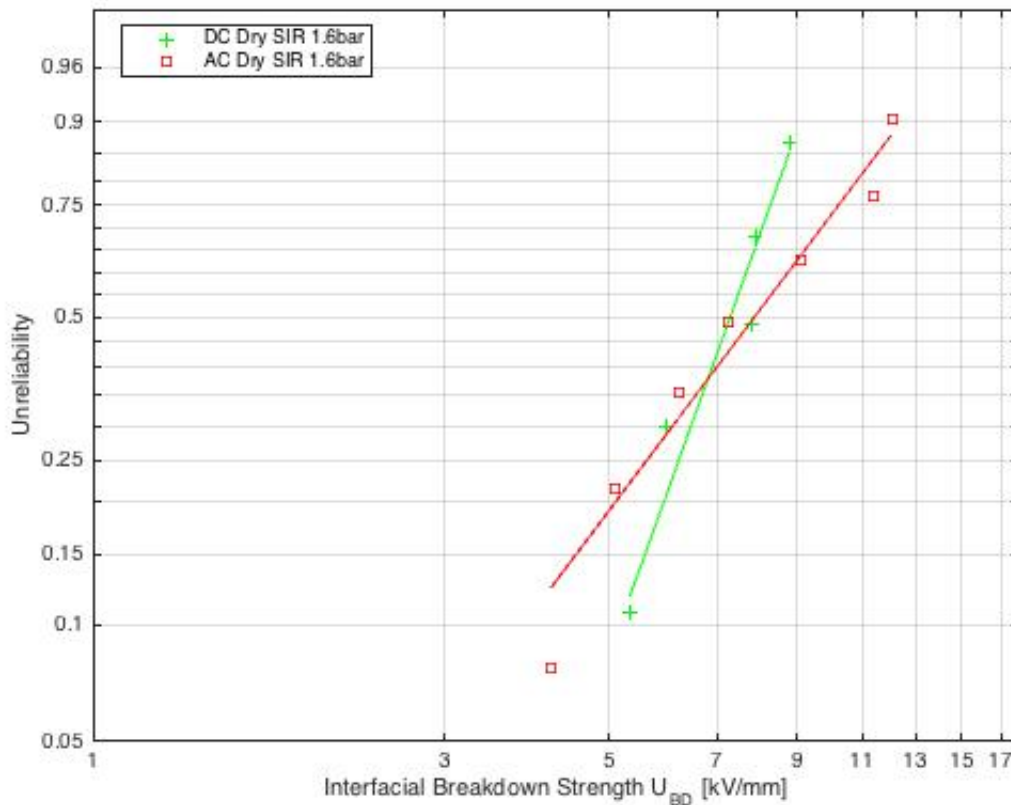


Figure 5.1: Weibull distribution of AC vs. DC under dry interface conditions

Table 5.1: AC vs. DC under dry interface conditions

	U63%	Slope	Min	Max	Mean
	[kV/mm]	a[/]	[kV/mm]	[kV/mm]	[kV/mm]
AC	9.04	2.5	4.18	12.06	7.91
DC	7.80	5.5	5.33	8.78	7.15

The figure 5.1 describing the Weibull distribution for dry interface i.e the voids are air filled.

The AC results has a larger distribution than the DC results. When testing the dielectric breakdown strength of an material one can assume that the same results occurs each time. This is not the case when increasing the voltage in steps until breakdown occurs, the breakdown will occur with a random variation each time. This can address the larger distribution for the AC breakdown results.

In theory the SiR interface with DC voltage applied should have a greater breakdown strength then with AC voltage applied. The experiments are run until breakdowns occurs, and it is partial discharges that contributes to the interfacial breakdown.

The AC breakdown strength is measured in RMS voltage, and is equal to the measured DC voltage. The amplitude voltage for AC is $\sqrt{2}$ higher than the measured RMS voltage. This means that the AC voltage is $\sqrt{2}$ higher than the DC voltage two times per period when it has reached its amplitude voltage. The degradation of the material will during AC be affected between the periods of the trigger voltage and the extinction voltage for both positive and negative half period with a voltage $\sqrt{2}$ higher than the AC RMS voltage and the DC voltage. This means that the PD activity for AC will start $\sqrt{2}$ times before the DC voltage.

The simulations in Comsol attached in appendix A.1 and A.2 shows a higher field strength in the air filled cavity were DC voltage is applied with a factor of $\sqrt{2}$. This caused by the difference in the ratio between permittivities and conductivities for SiR and air, shown in section 2.7.

These two findings will even out the difference between AC and DC, and will contribute to a breakdown strength in the same region for both AC and DC for dry interface conditions, like in the results.

5.3.2 Wet interface - AC vs. DC

In this section AC and DC results for wet interface condition are compared. From the graphical presentation in figure 5.2 the difference between the breakdown strength BDS is remarkable. The mean DC BDS is 3.4 times higher than the AC BDS.

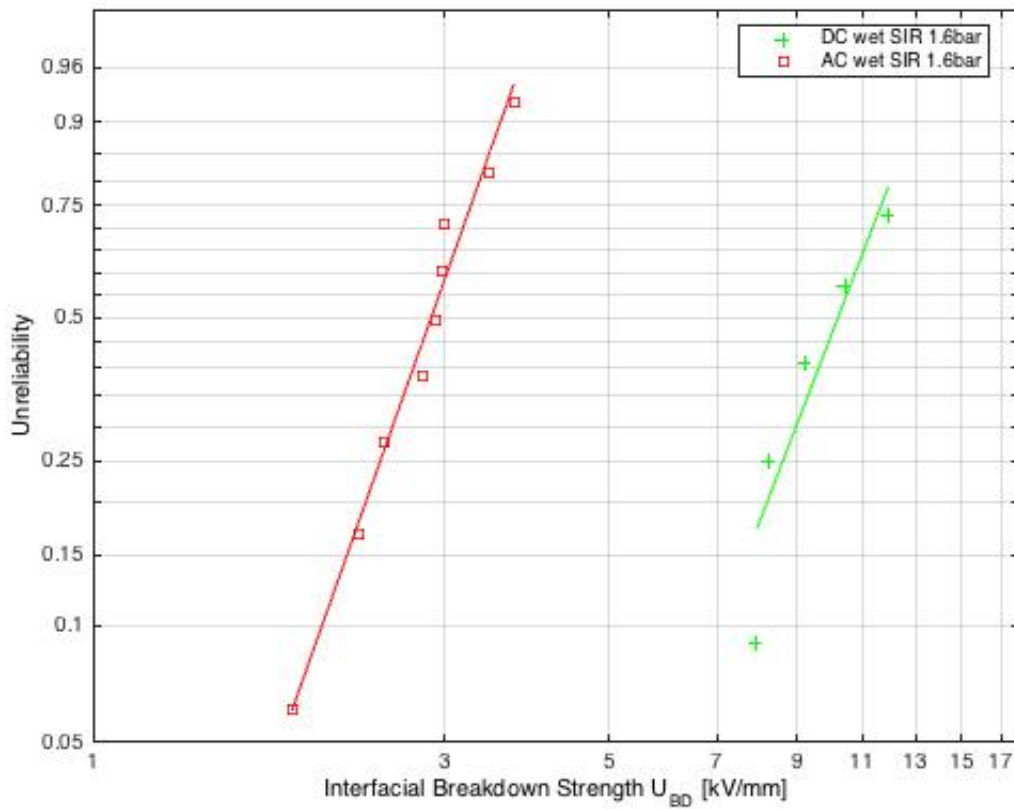


Figure 5.2: Weibull distribution of AC vs. DC under wet interface conditions

Table 5.2: AC vs. DC under wet interface conditions

	$U_{63\%}$ [kV/mm]	Slope a[/]	Min [kV/mm]	Max [kV/mm]	Mean [kV/mm]
AC	3.07	5.5	1.86	3.72	2.83
DC	10.96	5.1	7.93	11.94	9.57

For wet mating conditions there is impossible to fill all the voids with water during the mating process due to the SiRs hydrophobic qualities. This makes the voids in the interface partly air filled and partly water filled. This makes the interface connection existing of water filled voids in series with air filled voids and SiR contact spots. The water filled voids will act as contaminations at the interface connection providing high electric fields in at the transaction between the SiR contact spots and the water filled voids. The Comsol models in figures in [A.3](#) and [A.4](#) clearly shows this increment of the field strength in this section. The high field strength comes of the waters high conductivity both for AC and DC conditions.

Under AC conditions the high electric field arising at the surface of the water filled voids will contribute to a higher field inside the air filled voids. This contributes to PD activities at an earlier stage in the air filled voids. The polarity of the field will change two times each period, this contributes to heating, electrical treeing and rapidly degradation of the interface. All this contributes to lower breakdown strength for the wet interface condition for AC compared to DC.

Under DC conditions the polarity of the electric field will not change over time like under AC conditions. When applying the voltage by small increments the electric field will increase in correlation with the applied voltage with the same polarity. Under these conditions the enhanced field at the water filled voids surface will distribute in the surrounding SiR material causing a lower electric stress at the interface than under AC conditions.

Partial discharges is the mechanism that contributes to the breakdown. For AC conditions the discharge happens two times each period du to the changing polarity. This contributes to an rapidly degradation of the interface until breakdown occurs. For DC conditions the discharges do not come as rapidly as for AC conditions. PD under DC conditions uses much longer time to charge after an discharge ([17](#)). This contributes to the difference of 3.5 times as high breakdown strength for DC compared to AC under wet interface conditions.

5.3.3 Oily interface - AC vs. DC

Five trials were run. Only two of five trials an interfacial breakdown occurred. This was the same findings that Stip. Emre Kantar registered for his AC experiments. It is the design of the test rig that are causing the breakdown to occur along the outer surface of the SiR specimens from electrode to electrode. The oily interface condition is in the same area of electric strength as the test rig itself. This has to be improved before further experiments at this conditions can be examined.

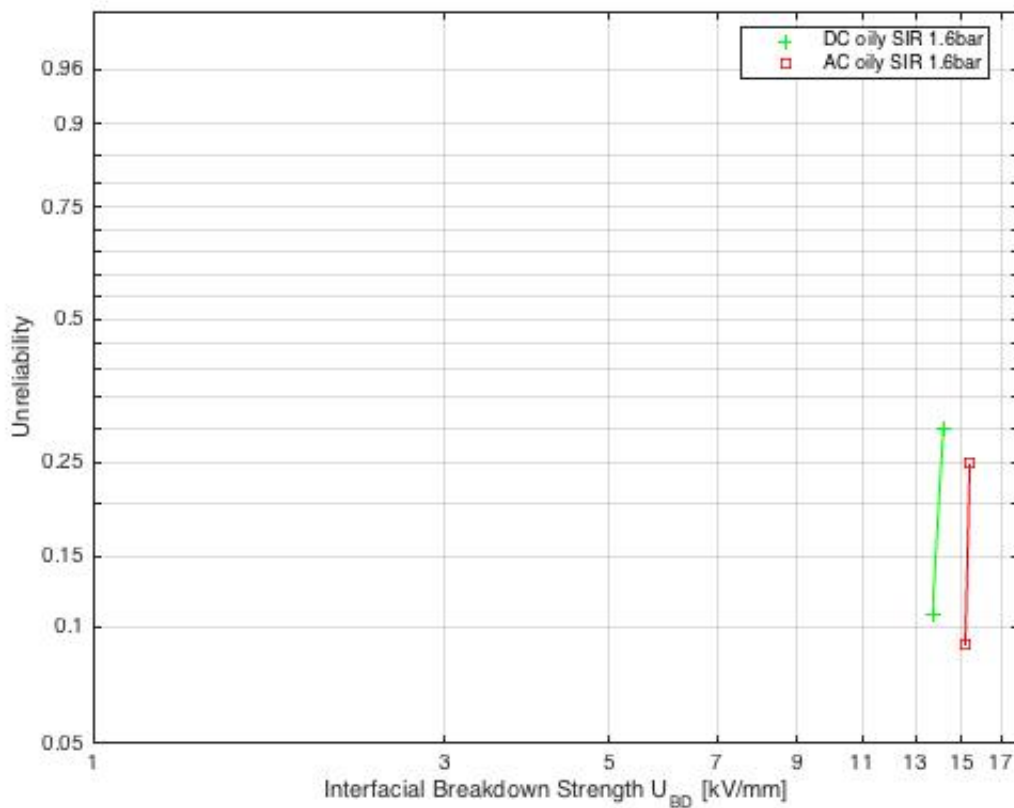


Figure 5.3: Weibull distribution of AC vs. DC under oily interface conditions

Table 5.3: AC vs. DC under oily interface conditions

	$U_{63\%}$ [kV/mm]	Slope a[/]	Min [kV/mm]	Max [kV/mm]	Mean [kV/mm]
AC	15.65	79.1	15.19	15.40	15.30
DC	14.62	33.4	13.70	14.12	13.94

For the oily interface condition the results showing a minor difference in the electric field strength for AC and DC voltage. This is expected according to the theory. From the Comsol simulations attached in appendix [A.5](#) and [A.6](#) it can be observed that for the oil filled void has a higher electric field strength for DC than for AC. This due to the ratio between the permittivities and conductivities for SiR and oil. The ratio for conductivity is 0.42 and for permittivity 1.34. So a higher field strength for DC is expected.

Since the difference between permittivities and conductivities are that small, the dielectric characteristics for both the oil and the SiR are quite similar. This contributes to low electric field enhancement at the surface of the spherical oil filled voids, that gives this interface condition such high electric field strength compared to the other conditions as dry and wet interface.

For oily interface condition 100% of the voids are oil filled. The oil and the SiR are such good dielectric materials that are quite similar. This leads to the high breakdown strength in the same area, only deviating due to minor differences between the permittivity and conductivity characteristics.

Chapter 6

Conclusion

An extensive study on the DC tangential electric breakdown strength of the interface between two solid insulation material made of SiR has been carried out. Over 300 experiment hours has been run examining the DC breakdown strength of SiR under dry, wet and oily interface conditions. The study also contains an experimentally approach of the elasticity modulus for the silicone rubber used in all the experiments. The main findings are presented as follows:

The elasticity modulus E for silicone rubber is measured to be $5.77[MPa]$. Two different methods gave results in the same region, making the experimentally approached value of elasticity modulus reliable.

The estimated breakdown voltage did not agree with the breakdown voltage results for dry interface conditions. The best fit result deviated by 37%. This by using the composite elasticity modulus with the largest deviation from the measured elasticity modulus and the elasticity modulus given by the manufacturer. The deviation between the result and the estimated BDV is to large to use the contact theory as reliable tool for calculating the estimated breakdown voltage for dry interface conditions.

The AC voltage reaches the ignition voltage for PD $\sqrt{2}$ times before the DC voltage. The difference between the simulated field strength inside the air filled void for DC are $\sqrt{2}$ higher than for AC. This will balance out the difference between the AC and DC making them reach the ignition voltage for PD at the same voltage. This contributes to a breakdown strength in

the same region for both AC and DC for dry interface conditions.

For wet mating conditions there is assumed there is impossible to fill all the voids with water during the mating process due to the SiRs hydrophobic qualities. This makes the voids in the interface partly air filled and partly water filled. The water filled voids will act as contaminations at the interface connection providing high electric fields in at the transaction between the SiR contact spots and the water filled voids. This contributes to PD activity at an earlier stage in the air filled voids. Under DC conditions the polarity of the electric field will not change over time like under AC conditions. Under these conditions the enhanced field at the water filled voids surface will distribute in the surrounding SiR material causing a lower electric stress at the interface than under AC conditions. This contributes to a breakdown strength 3.5 times higher for DC than for AC.

For oily interface condition 100% of the voids are oil filled. The oil and the SiR are such good dielectric materials that are quite similar. This leads to the high breakdown strength in the same area, only deviating due to minor differences between the permittivity and conductivity characteristics. This gives the oily interface condition a very strong tangential breakdown strength compared to the dry and wet conditions.

List of Figures

- 2.1 Build-up of a charge on a dielectric material showing a step up voltage at $t = 0$ and an electric breakdown at t_1 6
- 2.2 Example of a cross-section of the interface between two insulating materials showing cavities and contact spots. (2) 7
- 2.3 Model of the electric distribution along the interface displaying V_{void} and $V_{contact}$. (2) 8
- 2.4 Geometrical characteristics of a) a profile; b) an average section of the profile. 9
- 2.5 Simulated electric field distribution for air filled cavity at the SiR interface [kV/mm] 13
- 2.6 Appearance of partial discharges at geometrical constructions 14
- 2.7 Weibull presentation of AC electric breakdown strength with dry, wet and oily interface conditions 15

- 3.1 Experimental lab setup 19
- 3.2 Detailed illustration of test rig. 1: rectangular solid SiR specimens, 2: interface, 3: fixed electrode, 4: moving electrode, 5: spring, 6: wing nut, 7: high voltage wire, 8: earth wire, 9: weights, 10: moving weight-carrying plate, 11: guiding rods, 12: moving (upper) pressure dispersing block, 13: fixed (lower) pressure dispersing block, 14: supporting structure, 15: foundation.(6) 21
- 3.3 Electronic scale with raw SiR 23
- 3.4 Mixing SiR in vacuum chamber 23
- 3.5 Mold $4mm \times 500mm \times 500mm$ 23
- 3.6 Specimen $4mm \times 25mm \times 55mm$ 23
- 3.7 SiR specimens aligned to rotating disc 24
- 3.8 Grinding the specimens 24

3.9 Surface inspection	24
3.10 Specimens bulk	24
3.11 Test specimen nomenclature	26
3.12 Test specimen rectangulare	27
4.1 DC - Tangential electric breakdown strength under dry, wet and oily interface conditions	31
5.1 Weibull distribution of AC vs. DC under dry interface conditions	36
5.2 Weibull distribution of AC vs. DC under wet interface conditions	38
5.3 Weibull distribution of AC vs. DC under oily interface conditions	40
A.1 AC plot - Dry interface - Electric field strength [kV/mm]	50
A.2 DC plot - Dry interface - Electric field strength [kV/mm]	50
A.3 AC graph - Dry interface - Electric field strength [kV/mm]	51
A.4 DC graph - Dry interface - Electric field strength [kV/mm]	51
A.5 AC plot - Wet interface - Electric field strength [kV/mm]	52
A.6 DC plot - Wet interface - Electric field strength [kV/mm]	52
A.7 AC graph - Wet interface - Electric field strength [kV/mm]	53
A.8 DC graph - Wet interface - Electric field strength [kV/mm]	53
A.9 AC plot - Oily interface - Electric field strength [kV/mm]	54
A.10 DC plot - Oily interface - Electric field strength [kV/mm]	54
A.11 AC graph - Oily interface - Electric field strength [kV/mm]	55
A.12 DC graph- Oily interface - Electric field strength [kV/mm]	55

List of Tables

- 2.1 Surface roughness parameters 9
- 2.2 Material parameters, (7), (8), (9), (10), (11). 12
- 2.3 Comparison between dry, wet and oily interface at AC and DC conditions 15

- 3.1 Test parameters 20
- 3.2 Test specimen dimensions 26

- 4.1 Elasticity modulus test parameters and results using compression method 30
- 4.2 Elasticity modulus test parameters and results using tensile method 30
- 4.3 Estimated electric breakdown strength with respect to the composite elasticity modulus \hat{E} 30
- 4.4 DC - Dry, wet and oily interface conditions 31

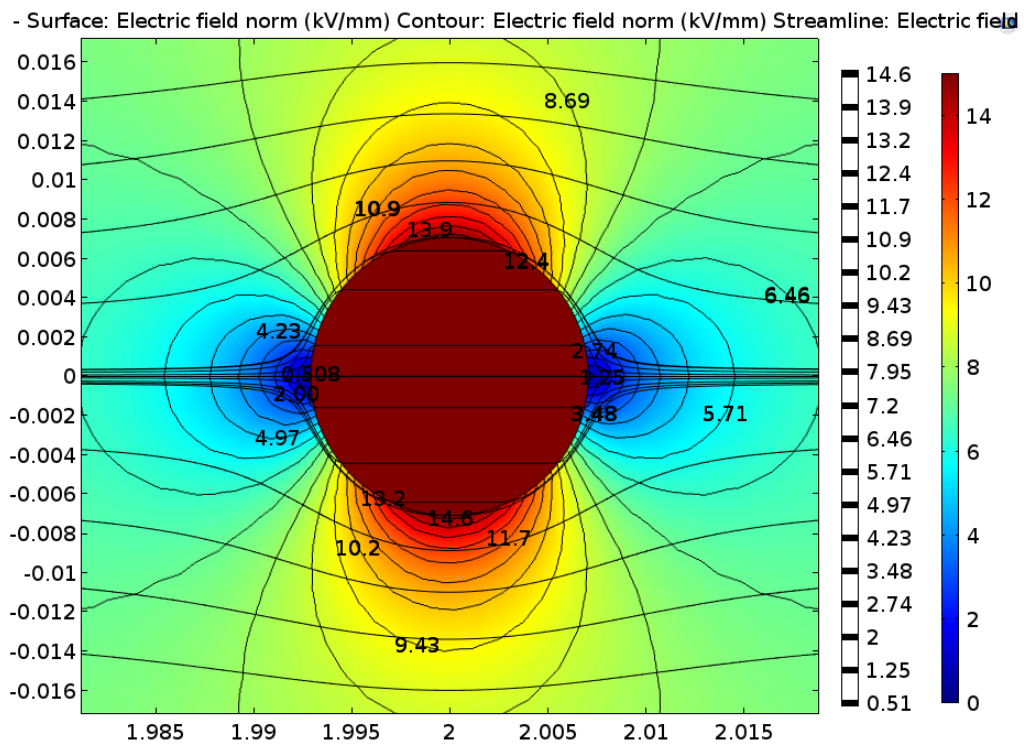
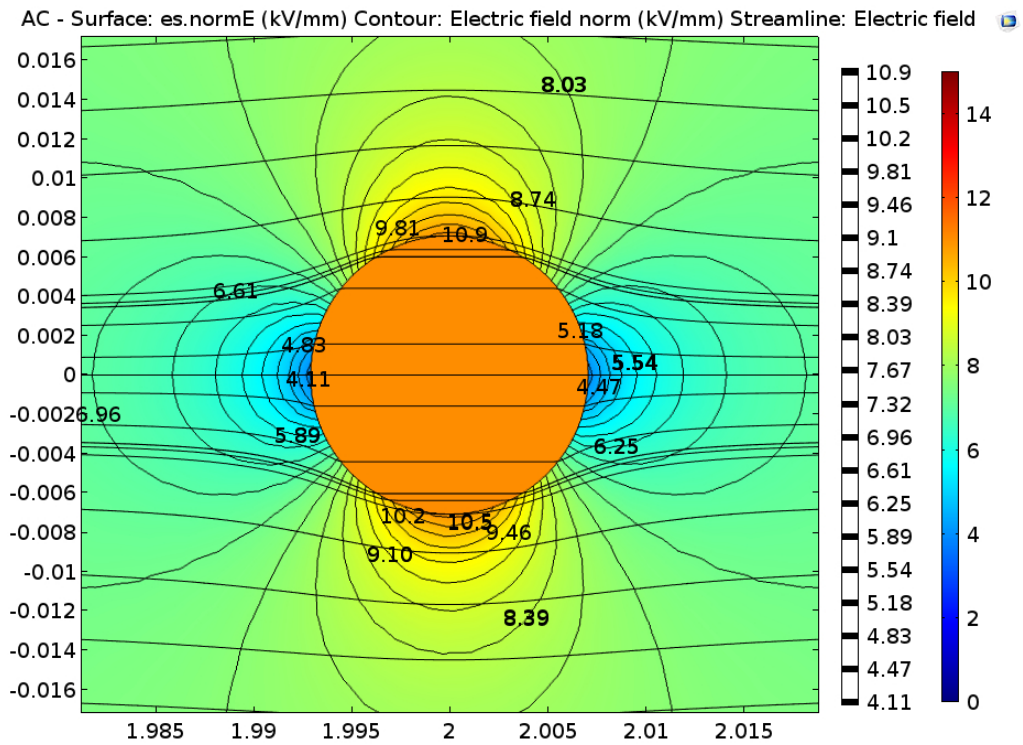
- 5.1 AC vs. DC under dry interface conditions 36
- 5.2 AC vs. DC under wet interface conditions 38
- 5.3 AC vs. DC under oily interface conditions 40

Appendix A

Electric field distribution simulations using Comsol Multiphysics 5.1

Comsol Multiphysics 5.1 is used to simulate the electric field strength for one cavity containing all three conditions, dry, wet and oily interface. The applied voltage is 30[kV] for both AC and DC. This for having the same foundation for comparison. All the graphs and plots are displayed with the same color and numbers scale, this also to make it easier for the reader to compare the results.

A.1 Dry interface conditions AC vs. DC plot



A.2 Dry interface conditions AC vs. DC graph

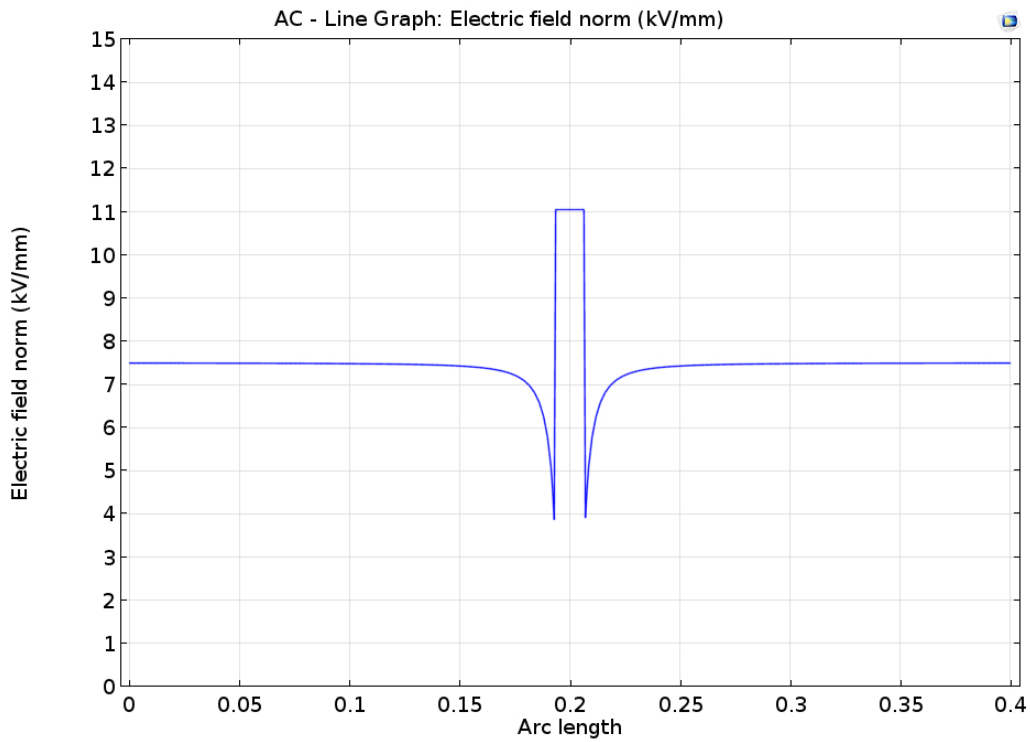


Figure A.3: AC graph - Dry interface - Electric field strength [kV/mm]

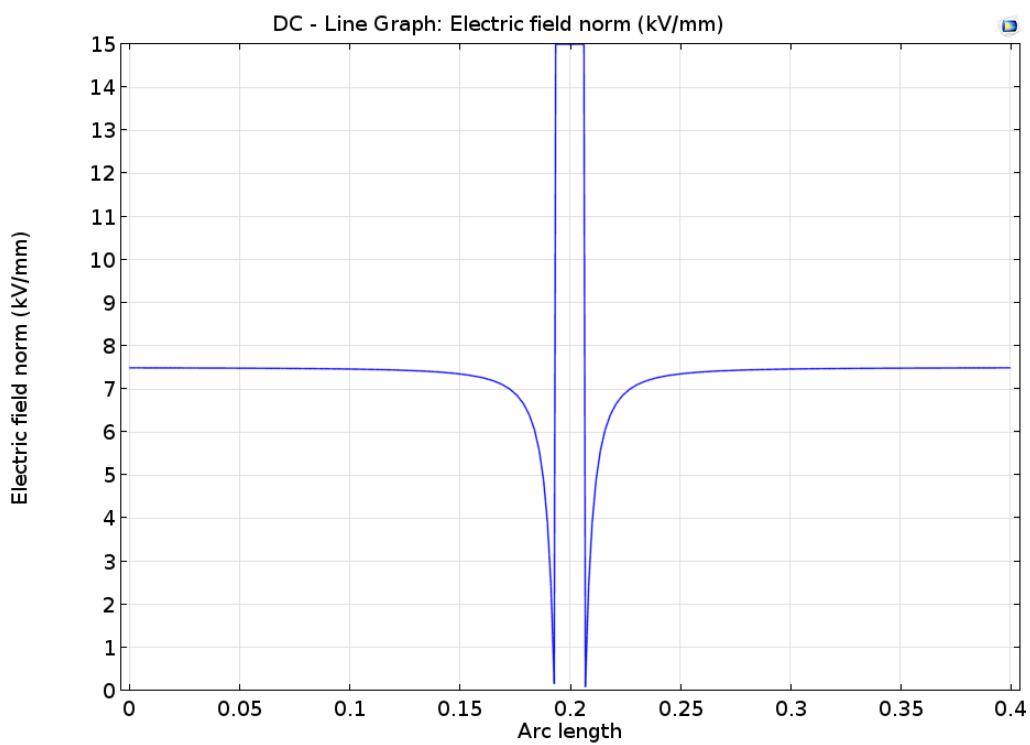


Figure A.4: DC graph - Dry interface - Electric field strength [kV/mm]

A.3 Wet interface conditions AC vs. DC plot

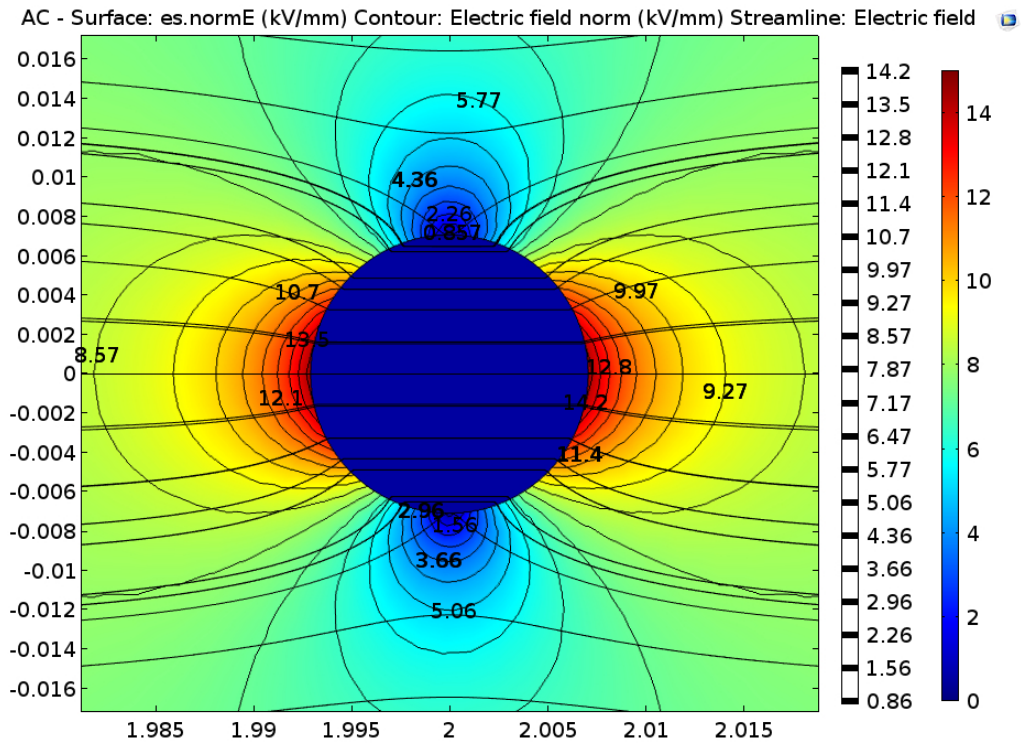


Figure A.5: AC plot - Wet interface - Electric field strength [kV/mm]

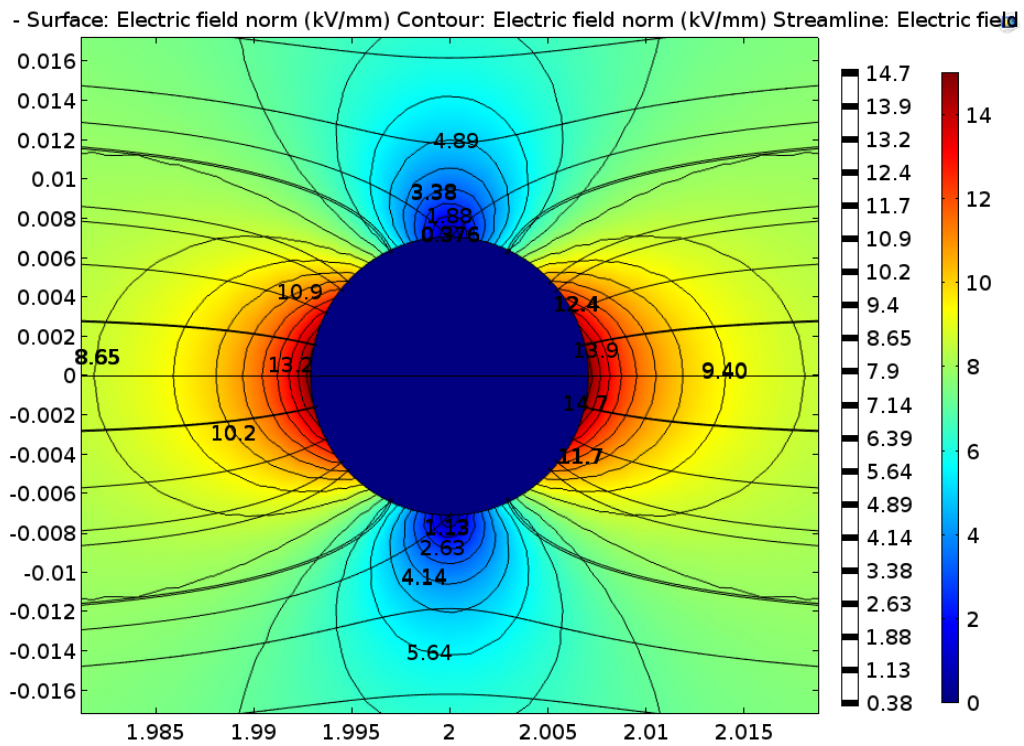


Figure A.6: DC plot - Wet interface - Electric field strength [kV/mm]

A.4 Wet interface conditions AC vs. DC graph

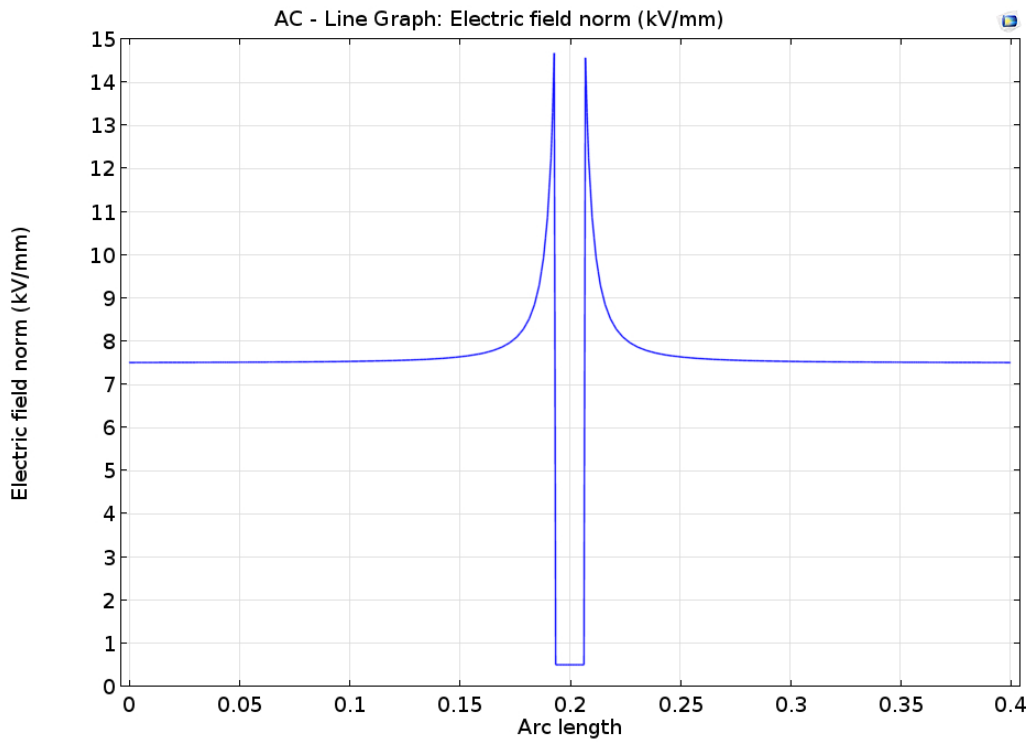


Figure A.7: AC graph - Wet interface - Electric field strength [kV/mm]

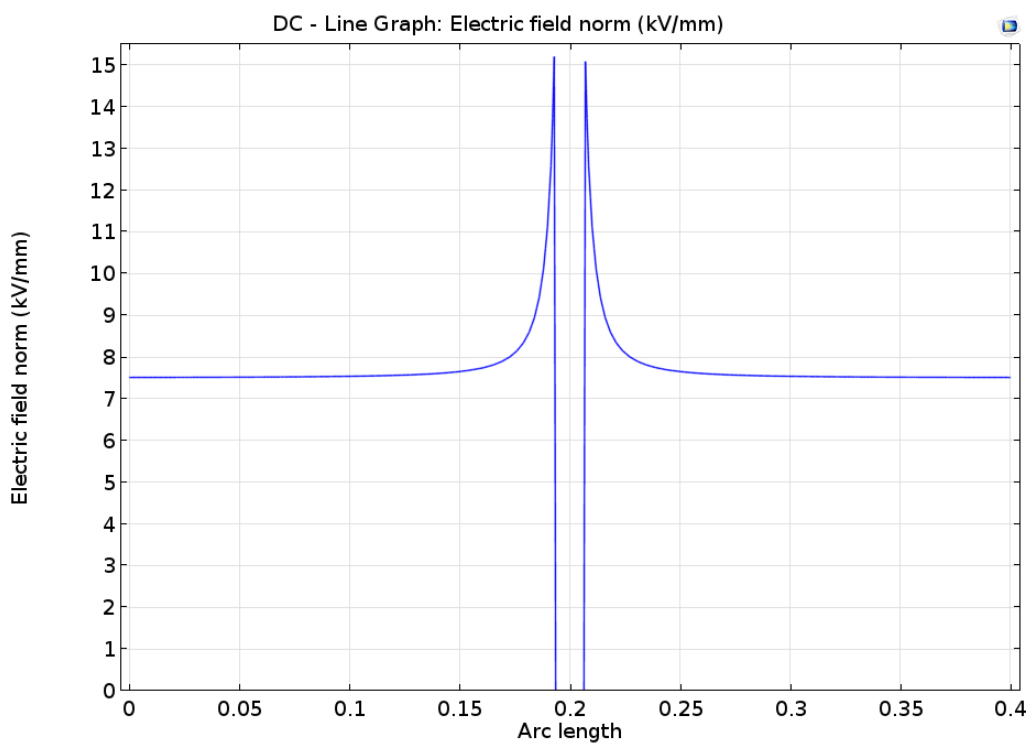


Figure A.8: DC graph - Wet interface - Electric field strength [kV/mm]

A.5 Oily interface conditions AC vs. DC plot

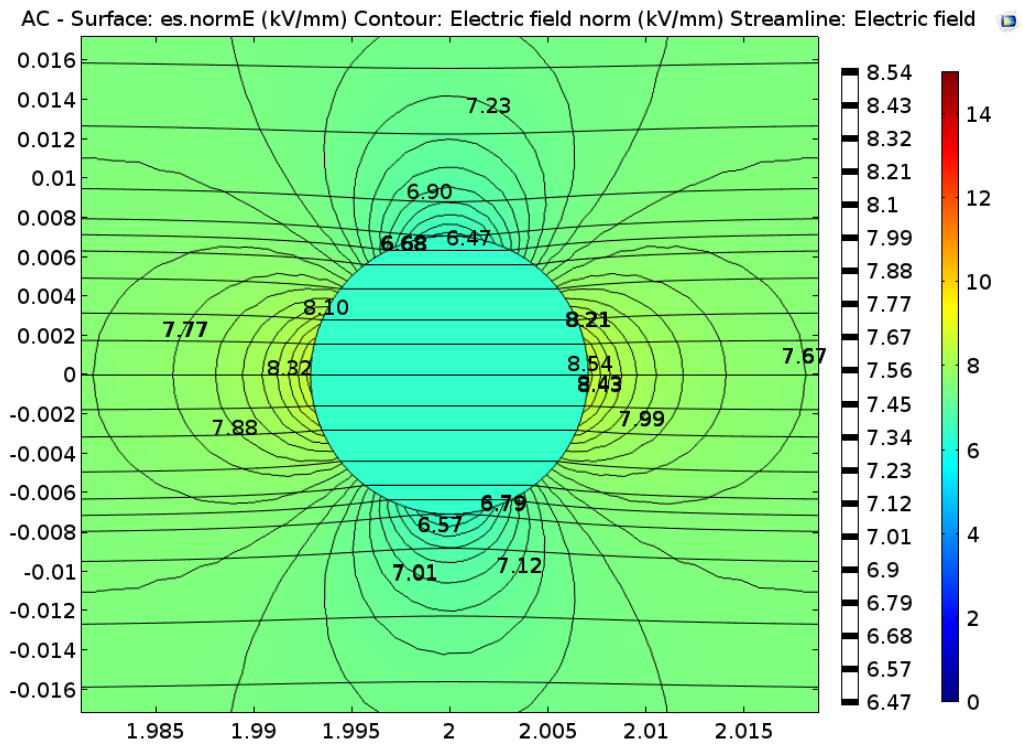


Figure A.9: AC plot - Oily interface - Electric field strength [kV/mm]

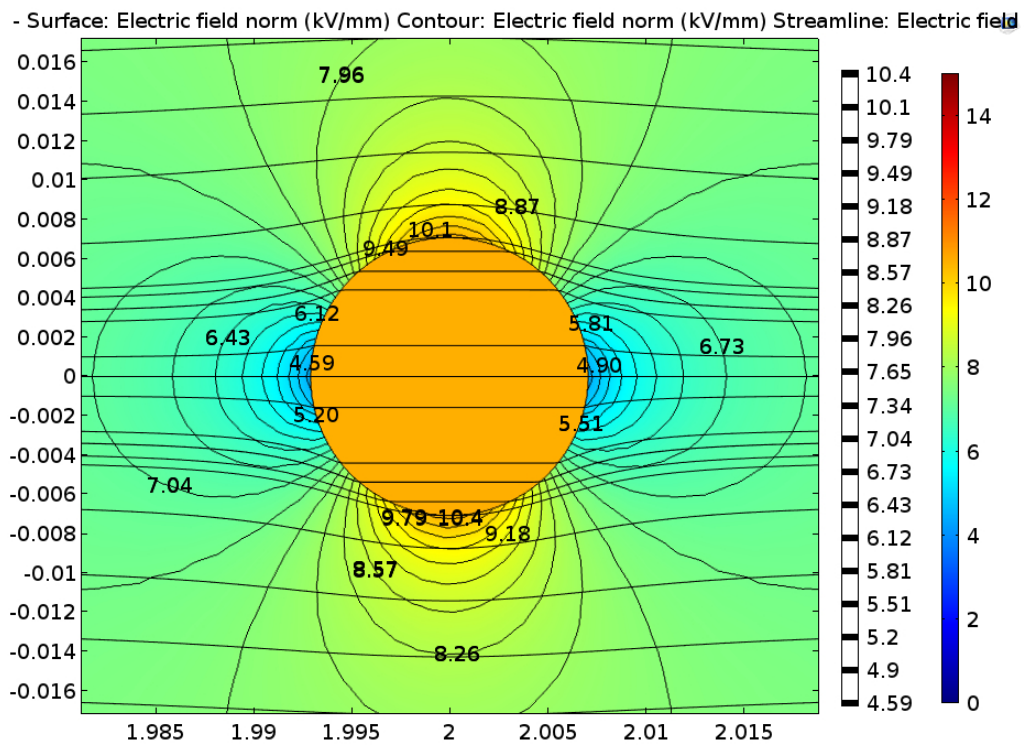


Figure A.10: DC plot - Oily interface - Electric field strength [kV/mm]

A.6 Oily interface conditions AC vs. DC graph

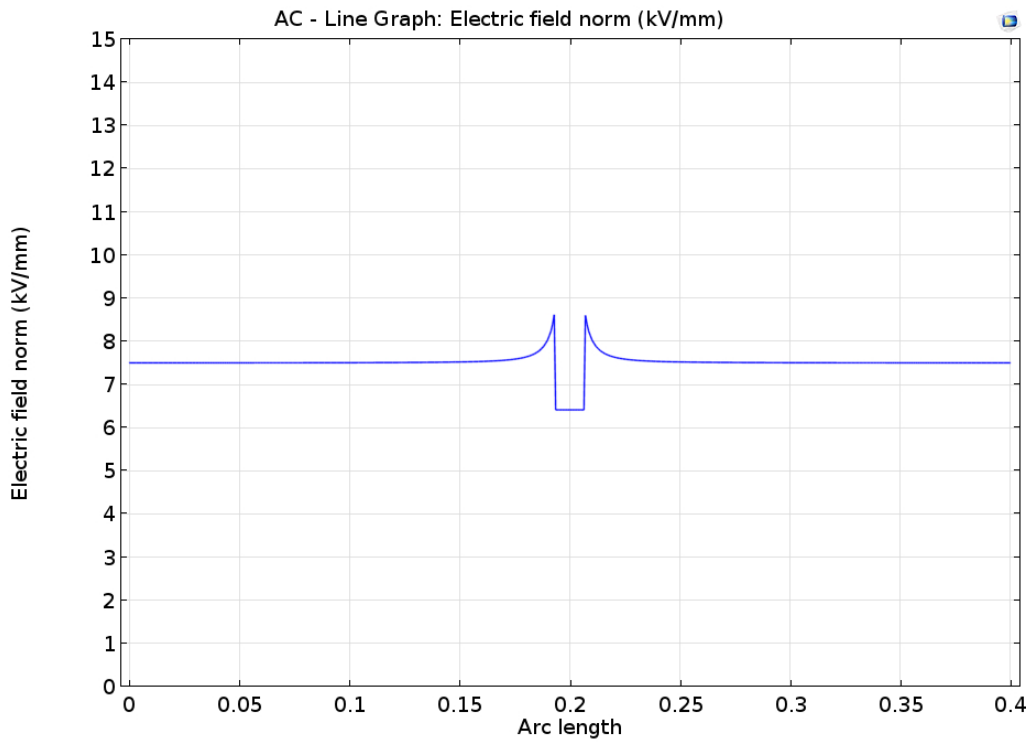


Figure A.11: AC graph - Oily interface - Electric field strength [kV/mm]

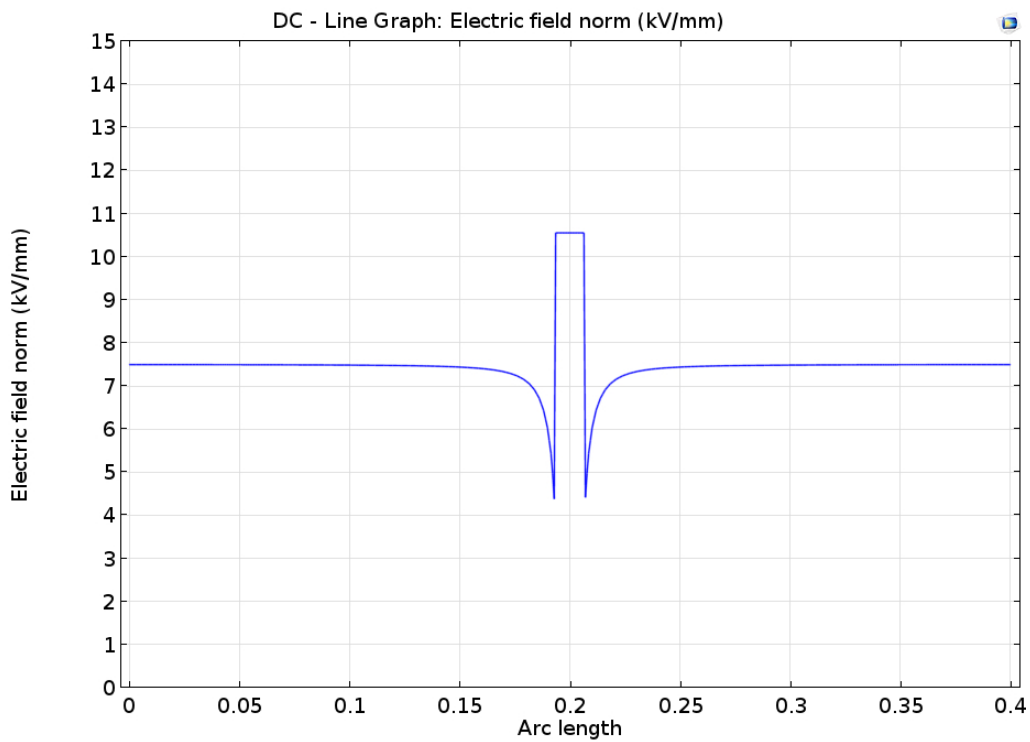


Figure A.12: DC graph- Oily interface - Electric field strength [kV/mm]

Bibliography

- [1] E. Ildstad, *TET4160 High Voltage Insulation Materials*. Department of Electric Power Engineering, 08 2014.
- [2] S. M. Hasheminezhad, "Breakdown strength of solid x2223; solid interfaces," in *PowerTech, 2011 IEEE Trondheim*, pp. 1–7, June 2011.
- [3] E. Kantar, "Modeling longitudinal breakdown strength of solid- solid interfaces using contact theory," 2016.
- [4] "Bruker contourgt, optical surface analysator," 20.05.16.
- [5] M. Hasheminezhad and E. Ildstad, "Application of contact analysis on evaluation of breakdown strength and pd inception field strength of solid-solid interfaces," *IEEE Transactions on Dielectrics and Electrical Insulation*, vol. 19, pp. 1–7, February 2012.
- [6] D. Panagiotopoulos, "Ac electrical breakdown strength of solid solid interfaces," Master's thesis, Delft University of Technology and Norwegian University of Science and Technology, October 2015.
- [7] J. Kolb, Y. Minamitani, S. Xiao, X. Lu, M. Laroussi, R. P. Joshi, K. H. Schoenbach, E. Schamiloglu, and J. Gaudet, "The permittivity of water under high dielectric stress," in *Pulsed Power Conference, 2005 IEEE*, pp. 1266–1269, June 2005.
- [8] <http://www.wacker.com/cms/en/products/product/product.jsp?product=11663>, "Sirelastosil lr 3003/60 a/b by wacker silicones," 20.05.16.
- [9] http://www.midel.com/productsmidel/midel_7131, "Midel 7131 synthetic ester," 20.05.16.

- [10] <http://chemistry.about.com/od/moleculescompounds/a/Table-Of-Electrical-Resistivity-And-Conductivity.htm>, "Table of electrical resistivity and conductivity," 20.05.16.
- [11] <http://www.azom.com/properties.aspx?ArticleID=920>, "Table of young's modulus for silicon rubber," 20.05.16.
- [12] E. Kantar, D. Panagiotopoulos, and E. Ildstad, "Factors influencing the tangential ac breakdown strength of solid-solid interfaces," 2015.
- [13] E. Kantar, F. Mauseth, and E. Ildstad, "Effect of pressure and elastic modulus on tangential breakdown strength of solid-solid interfaces," 2016.
- [14] "Struers occilating grinder," 20.05.16.
- [15] O. A. Hamemerøy, "Dc electrical breakdown strength of solid solid silicon rubber interfaces," tech. rep., Norwegian University of Science and Technology, 12 2015.
- [16] <http://www.azom.com/properties.aspx?ArticleID=920>, "Lloyd lr5k, machine for tensile and compresion testing," 20.05.16.
- [17] P. K. Olsen, F. Mauseth, and E. Ildstad, "The effect of dc superimposed ac voltage on partial discharges in dielectric bounded cavities," in *High Voltage Engineering and Application (ICHVE), 2014 International Conference on*, pp. 1–4, Sept 2014.